







# Manipulating exudate composition from root apices shapes the microbiome throughout the root system

Akitomo Kawasaki <sup>1,†</sup>, Paul G. Dennis,<sup>2</sup> Christian Forstner,<sup>2</sup> Anil K. H. Raghavendra,<sup>2,†</sup>  
Ulrike Mathesius <sup>3</sup>, Alan E. Richardson <sup>1</sup>, Emmanuel Delhaize,<sup>1,3</sup> Matthew Gilliham <sup>4</sup>,  
Michelle Watt <sup>5</sup> and Peter R. Ryan <sup>1,†,\*</sup>

1 CSIRO Agriculture and Food, Canberra, ACT 2601, Australia

2 Faculty of Sciences, School of Earth and Environmental Sciences, The University of Queensland, St Lucia, QLD 4072, Australia

3 Division of Plant Sciences, Research School of Biology, Australian National University, Canberra, ACT 2601, Australia

4 ARC Centre of Excellence in Plant Energy Biology, School of Agriculture, Food and Wine, Waite Research Institute, University of Adelaide, Glen Osmond, SA 5064, Australia

5 School of BioSciences, University of Melbourne, Parkville, VIC 3010, Australia

\*Author for communication: peter.ryan@csiro.au

†Present address for AK and AKHR: NSW Department of Primary Industries, Elizabeth Macarthur Agricultural Institute, Menangle, NSW 2568, Australia

‡Senior author.

All authors conceived the original research plans; P.R.R. and A.K. supervised the experiments; E.D. generated the NILs; A.K. performed the sterile growth methods and A.K. performed the soil experiments and collected tissues with assistance from P.R.R.; A.K. prepared the DNA preps and P.G.D. and A.K.H.R. sequenced the amplicons; A.K. and P.R.R. analyzed the data and statistical analyses were performed by C.F., A.K., and P.G.D.; All authors contributed to the article.

The author(s) responsible for distribution of materials integral to the findings presented in this article in accordance with the policy described in the Instructions for Authors (<https://academic.oup.com/plphys/pages/General-Instructions>) are: Peter R. Ryan (peter.ryan@csiro.au) and Akitomo Kawasaki (aki.kawasaki@dpi.nsw.gov.au).

## Abstract

Certain soil microorganisms can improve plant growth, and practices that encourage their proliferation around the roots can boost production and reduce reliance on agrochemicals. The beneficial effects of the microbial inoculants currently used in agriculture are inconsistent or short-lived because their persistence in soil and on roots is often poor. A complementary approach could use root exudates to recruit beneficial microbes directly from the soil and encourage inoculant proliferation. However, it is unclear whether the release of common organic metabolites can alter the root microbiome in a consistent manner and if so, how those changes vary throughout the whole root system. In this study, we altered the expression of transporters from the *ALUMINUM-ACTIVATED MALATE TRANSPORTER* and the *MULTIDRUG AND TOXIC COMPOUND EXTRUSION* families in rice (*Oryza sativa* L.) and wheat (*Triticum aestivum* L.) and tested how the subsequent release of their substrates (simple organic anions, including malate, citrate, and  $\gamma$ -amino butyric acid) from root apices affected the root microbiomes. We demonstrate that these exudate compounds, separately and in combination, significantly altered microbiome composition throughout the root system. However, the root type (seminal or nodal), position along the roots (apex or base), and soil type had a greater influence on microbiome structure than the exudates. These results reveal that the root microbiomes of important cereal species can be manipulated by altering the composition of root exudates, and support ongoing attempts to improve plant production by manipulating the root microbiome.

## Introduction

Roots alter the physical and chemical properties of the soil immediately surrounding them. One of the most important drivers of these changes is rhizodeposition, which encompasses all materials released and shed from roots, including water-soluble exudates, sloughed-off cells, mucilages, dead tissues, and gases. Microorganisms in the soil able to utilize these organic substrates tend to proliferate on the roots and rhizosphere (Bais et al., 2006). Therefore, the structure of the microbial communities near roots will depend, in part, on the composition of exudates and other rhizodeposits (Bulgarelli et al., 2012, 2015; Chaluvadi and Bennetzen, 2018).

A small proportion of microorganisms in the rhizosphere can benefit the host plant by improving nutrient availability, suppressing the colonization of pathogens, or by releasing compounds with phytohormone-like activity that stimulates growth (Beneduzi et al., 2012; Chaluvadi and Bennetzen, 2018; Kudoyarova et al., 2019; Mohanram and Kumar, 2019). Strategies that encourage the proliferation of these beneficial microorganisms can potentially boost productivity without the use of agrochemicals (Vessey, 2003; Ryan et al., 2009a). Rhizobia, mycorrhizal fungi, and *Trichoderma* are examples of plant growth-promoting rhizobacteria and beneficial fungi that are already utilized in agriculture and horticulture. They are usually applied by inoculating the soil or coating the seed prior to sowing (Deaker et al., 2004; Thapa et al., 2020). However, the success of these “biologicals” is inconsistent and often short-lived because competition with other microorganisms or unfavorable soil conditions can negatively impact their persistence in soil and around roots (Castro-Sowinski et al., 2007).

An alternative strategy for manipulating the root microbiome, and one that could complement current practices, utilizes root exudates to recruit microorganisms from the bulk soil and/or promote the proliferation of inoculants (Wu et al., 2018). The advantages of this approach are: (1) exudates are deposited at the root-soil interface where they are most likely to impact microbial growth; (2) varying the composition of exudates can alter the structure of the root microbiome; (3) the release of substrates throughout the host's lifecycle will maintain selection pressure on the microbial communities; and (4) conventional breeding methods or biotechnology can be used to alter the composition of exudates either by changing the expression of transporter proteins or metabolic pathways (Delhaize et al., 2007; Badri et al., 2008).

Previous studies have provided a proof-of-principle that root exudates, and especially secondary metabolites like flavonoids and triterpenes, can shape the microbial communities near roots (Soedarjo and Borthakur, 1996; Oger et al., 2004; Badri et al., 2008; White et al., 2017; Stringlis et al., 2018; Cotton et al., 2019; Huang et al., 2019; Koprivova et al., 2019; Voges et al., 2019). What has not been investigated in these studies, or elsewhere, is whether the changes are uniform over the whole root system or restricted to certain regions. Moreover, most root exudates are not complex secondary metabolites but low molecular weight compounds

such as sugars, organic acids, and amino acids that are ready sources of nutrition for many microorganisms (Bacilio-Jiménez et al., 2003; Walker et al., 2003a, 2003b; Wang et al., 2006; Oburger et al., 2009; Tawaraya et al., 2014; Kawasaki et al., 2016; Mönchgesang et al., 2016; Warren, 2016; Kawasaki et al., 2018). Previous studies that have attempted to link these exudates with changes to the root microbiome (Tsfaye et al., 2003; Rudrappa et al., 2008) have not examined the spatial variation of these changes.

This study used rice (*Oryza sativa* L.) and wheat (*Triticum aestivum* L.) lines that vary in the expression of transporters encoded by the ALUMINUM-ACTIVATED MALATE TRANSPORTER (ALMT) and the MULTIDRUG AND TOXIC COMPOUND EXTRUSION (MATE) families. We chose these transporters because the substrates they release from roots are common metabolites that are present in all plant cells. This means that the outcomes from these studies are likely to be relevant to other plant species. One of these transporters in wheat is encoded by *TaALMT1*, which was initially characterized as an aluminum ( $\text{Al}^{3+}$ )-tolerance gene (Sasaki et al., 2004).  $\text{Al}^{3+}$  toxicity is the main factor limiting plant production on acidic soils because these cations inhibit root growth at low concentrations (Kinraide and Parker, 1989; Kochian, 1995). The  $\text{Al}^{3+}$  tolerance of some plant species, and the considerable intraspecific variation in tolerance displayed, often relies on the release of simple organic anions (malate and citrate) from the root apices that bind with, and detoxify, the harmful  $\text{Al}^{3+}$  (Ma et al., 2001; Ryan and Delhaize, 2010). *TaALMT1* encodes an anion channel that is expressed in the root apices of wheat roots and the protein is activated by the  $\text{Al}^{3+}$  cations present in acidic soils to release malate,  $\gamma$ -amino butyric acid (GABA), and other substrates (Sasaki et al., 2004; Piñeros et al., 2008; Zhang et al., 2008; Kawasaki et al., 2018; Ramesh et al., 2018). *TaMATE1B* controls a second mechanism for  $\text{Al}^{3+}$  tolerance in wheat. It encodes a citrate transporter from the MATE family, and a naturally occurring mutation in some genotypes results in a constitutive release of citrate from the root apices (Ryan et al., 2009b; Tovkach et al., 2013). Prior to this study, citrate release via *TaMATE1B* had only been confirmed from the seminal roots of young wheat seedlings. *OsALMT4* is a member of the ALMT family of anion channels in rice, and transgenic lines over-expressing *OsALMT4* display a constitutive release of malate and other substrates from the roots (Liu et al., 2017, 2018).

This study examined whether the microbial communities on the roots of rice and wheat can be manipulated in a consistent manner by altering the activity of membrane transporters and the release of organic exudates. We also assessed how exudates from the root apices shifted the microbiome structure throughout the root system.

## Results

The aims of each experiment in this study and a description of the plant materials used are summarized in Table 1.

**Table 1** Aims of each experiment listing the transporters, plant genotypes and likely root exudate substrates released in each soil

Exp.	Aim	Plant Species	Genotypes	Soil	Main Substrates Released from the Active Transporters in Each Soil	Comments
I	To test whether citrate release via TaMATE1B occurs from the apices of seminal axile roots only or from all root types.	Wheat	<i>NIL-TaMATE1B</i> <i>NIL-null</i>	Hydroponics Hydroponics	Citrate None	TaMATE1B facilitates the constitutive release of citrate from seminal axile roots, but whether this also occurs from other roots is unknown.
II	To test the effect of OsALMT4 activity on the root microbiome in rice.	Rice	<i>OX-OsALMT4</i> <i>OX-null</i>	Yellow Chromosol Yellow Chromosol	Malate, GABA* None	Constitutive release of substrates occurs from the root apices of the transgenic line <i>OX-OsALMT4</i> but not from <i>OX-null</i> .
III	To test the effect of TaALMT1 activity on the microbiome of wheat seminal roots.	Wheat	<i>NIL-null</i>	Ferrosol	Malate, GABA	The Al <sup>3+</sup> in the unamended Ferrosol will activate TaALMT1 activity and release substrates from the root apices.
				Ferrosol + gypsum	None	The Al <sup>3+</sup> in the gypsum-amended Ferrosol is too low to activate TaALMT1 function, and no substrates are released. (See <a href="#">Supplemental Figure S2</a> )
IV	To test the effect of TaMATE1B on the root microbiome, with and without TaALMT1 activity.	Wheat	<i>NIL-TaMATE1B</i> <i>NIL-null</i>	Red Chromosol	Citrate	In the Red Chromosol, citrate release occurs from <i>NIL-TaMATE1B</i> , but not from <i>NIL-null</i> . No malate release occurs from either.
				Red Chromosol	None	
			<i>NIL-TaMATE1B</i>	Ferrosol	Malate, GABA and citrate	The Al <sup>3+</sup> in the Ferrosol will activate TaALMT1 in both <i>NIL-TaMATE1B</i> and <i>NIL-null</i> , while citrate release occurs only from <i>NIL-TaMATE1B</i> .

\*Note that GABA release has not been measured directly from the roots of *OX-OsALMT4* plants, but this is predicted from other reports.

### Citrate release and TaMATE1B expression in various root types of wheat

We first used the near-isogenic wheat (*T. aestivum* L.) lines *NIL-null* and *NIL-TaMATE1B* to test whether citrate exudation via TaMATE1B occurs only from seminal roots of wheat or from other root types as well. Root exudates were collected from the apices of seminal axile roots, laterals of seminal roots, nodal axile roots, and laterals of nodal roots. For *NIL-null* plants, citrate exudation from the seminal and nodal axile root apices was low,  $\sim 10$  pmol root apex<sup>-1</sup> h<sup>-1</sup>, and exudation from the laterals was  $\sim 4$  pmol root apex<sup>-1</sup> h<sup>-1</sup> (Figure 1A). In contrast, citrate exudation from *NIL-TaMATE1B* was  $\sim 140$  pmol root apex<sup>-1</sup> h<sup>-1</sup> for the seminal and nodal axile roots, and  $\sim 20$  pmol root apex<sup>-1</sup> h<sup>-1</sup> for the lateral roots (Figure 1A). Since the average diameter of lateral roots ( $\sim 0.25$  mm) was smaller than the main axile roots ( $\sim 0.75$  mm), these rates were normalized for tissue volume. After this conversion, the exudation from all root apical tissues of *NIL-TaMATE1B* was similar, at  $\sim 70$  pmol mm<sup>-3</sup> root section h<sup>-1</sup> (Figure 1B). Root tissue was also collected from the base of seminal axile roots and nodal axile roots of *NIL-TaMATE1B* plants (avoiding lateral roots) to measure citrate release from those tissues. Citrate release from the basal root tissue was  $< 10$  pmol root section<sup>-1</sup> h<sup>-1</sup>, confirming that citrate exudation predominantly occurs from the root apices. Expression levels of the *TaMATE1* family reflected the pattern of citrate efflux and were

significantly greater in *NIL-TaMATE1B* tissues than *NIL-null* for all root types (Supplemental Figure S1).

### Effect of OsALMT4 activity on the root microbiome in rice

The transgenic rice (*O. sativa* L.) line *OX-OsALMT4* shows constitutive release of malate from its root apices while the null sister line, *OX-null*, shows little or no malate release (Liu et al., 2017). These plants were grown for 8 d in soil and the bacterial communities colonizing the root apices and root bases were compared. The null hypothesis tested was that OsALMT4 activity does not affect the microbiome along the roots of rice seedlings (Table 1).

Detrended correspondence analysis (DCA) of the bacterial community structures and pairwise comparisons of the different samples using a multivariate generalized linear model (GLM) with the *mvabund* package in R showed that communities collected from the root apices and bases were significantly different from each other, and both were different from the bulk soil ( $P < 0.005$ ; Figure 2A). Members of the Actinobacteria, Betaproteobacteria, and Bacilli were more abundant on the roots than the bulk soil, while the Acidobacteria, Alphaproteobacteria, Gemmatimonadetes, and Chloroflexi JG37-AG-4 were more abundant in the bulk soil (Figure 2B).

The effect of OsALMT4 activity on the root microbiome was obtained by comparing samples from *OX-OsALMT4* and

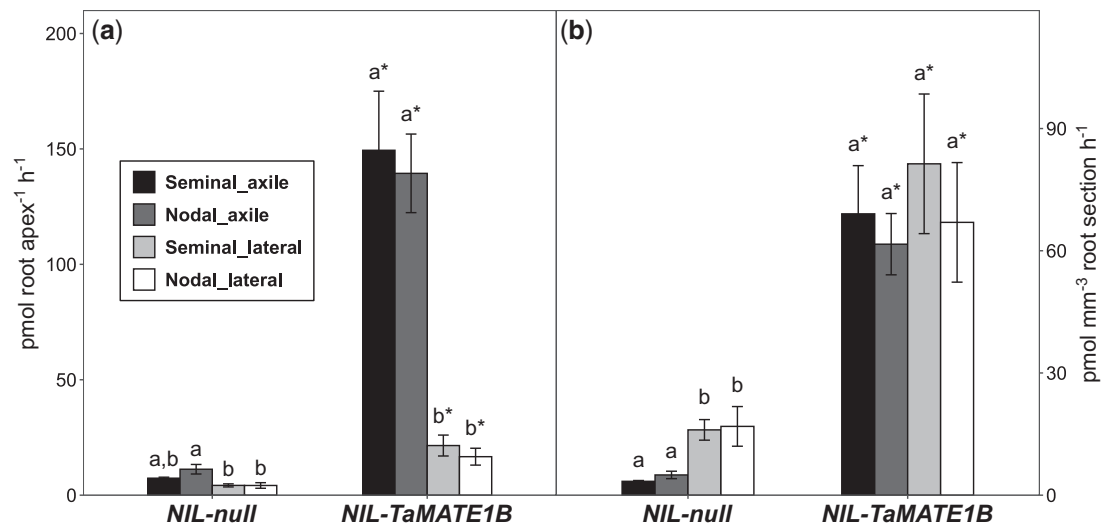


**Figure 1** Citrate efflux from the apices of different root types of wheat. *NIL-null* or *NIL-TaMATE1B* plants were grown in sterile hydroponic conditions and exudates were collected from various root tissues (Experiment I). Data are presented as (A) citrate efflux per root apex, and (B) citrate efflux normalized to the tissue volume ( $\text{mm}^3$ ) (means  $\pm$  standard error ( $\text{SE}$ ),  $n = 5$ ). Lowercase letters above the bars indicate differences ( $P < 0.05$ ) between the different tissues for the *NIL-null* or *NIL-TaMATE1B* lines, while asterisks above the *NIL-TaMATE1B* bars indicate the efflux from *NIL-TaMATE1B* is significantly greater ( $P < 0.05$ ) than the corresponding tissue from *NIL-null*. Data were transformed to natural log prior to two-way analysis of variance (ANOVA) with Tukey's post-hoc test.

*OX-null*. We found that the bacterial communities colonizing the root apices of *OX-OsALMT4* were significantly different from *OX-null* plants ( $mvabund P = 0.02$ ), and the communities colonizing the root bases of *OX-OsALMT4* were also significantly different from *OX-null* plants ( $mvabund P = 0.006$ ). However, the changes associated with *O*sALMT4 activity were much smaller than the differences between the root apices and root bases. *DESeq2* analyses identified the individual operational taxonomic units (OTUs) showing significant differences in abundance between the two plant genotypes (Figure 3). Eight OTUs from the Betaproteobacteria (Genus *Burkholderia/Paraburkholderia*) and two from the Actinobacteria (OTU29, *Leifsonia*; OTU45, *Pseudarthrobacter*) were more abundant in *OX-OsALMT4* compared with *OX-null* at both the root apices and the root bases. In contrast, eight Bacilli OTUs were more abundant at the bases of *OX-null* compared with *OX-OsALMT4* (Figure 3B), and one of these (OTU78; uncultured *Sporosarcina*) was also enriched at the root apices of *OX-null*. A detailed description of these OTUs is provided in Supplemental Table S1. These results indicate that *O*sALMT4 activity at the root apices significantly affected the bacterial microbiome along rice roots and therefore the null hypothesis was rejected.

### Effect of TaALMT1 activity on the root microbiome of wheat

The wheat genotype *NIL-null* was grown on two similar but contrasting soils: a Ferrosol and the same Ferrosol amended with gypsum. The high concentration of  $\text{Al}^{3+}$  in the Ferrosol activates the TaALMT1 channel to release malate and other substrates from the root apices, whereas the much lower  $\text{Al}^{3+}$  concentration in the gypsum-amended Ferrosol will not activate TaALMT1 (Table 1). The relative

toxicity of these soils was confirmed in preliminary experiments (Supplemental Figure S2). The bacterial and fungal microbiomes were characterized at the apices and bases of seminal roots and compared between the two soils. The null hypothesis was that TaALMT1 activity does not affect the bacterial or fungal microbiomes along seminal roots.

Final shoot biomass of plants from the Ferrosol and amended Ferrosol is shown in Supplemental Figure S3. DCA plots of the microbiomes indicated that the largest differences in bacterial and fungal communities existed between the bulk soil samples and the root bases, while communities on the root apices fell between these extremes (Figure 4). The addition of gypsum to the Ferrosol caused a small but significant shift in the bacterial and fungal communities in the bulk soil samples ( $mvabund P < 0.005$ ). The influence of TaALMT1 activity on the root microbiomes was determined by comparing root samples collected from the Ferrosol (TaALMT1 is activated) and the gypsum-amended Ferrosol (TaALMT1 is not activated). The microbial communities colonizing the root apices of plants from the Ferrosol were significantly different from plants grown in the amended Ferrosol. Similarly, the communities colonizing the root bases of plants from the Ferrosol were significantly different from plants grown in the amended Ferrosol ( $mvabund P < 0.005$  for all comparisons; Figure 4).

The OTUs showing significant differences in abundance on root samples from the Ferrosol compared with the amended Ferrosol are shown in Figure 5. For the bacteria, six OTUs closely matching *Peptoclostridium difficile* (Class Clostridia) and others from the Genera *Arthrobacter*, *Massilia*, and *Alkanindiges* were more abundant at the apices of roots from the Ferrosol (Figure 5A; Supplemental Table S2). In contrast, eight OTUs, mostly from Classes



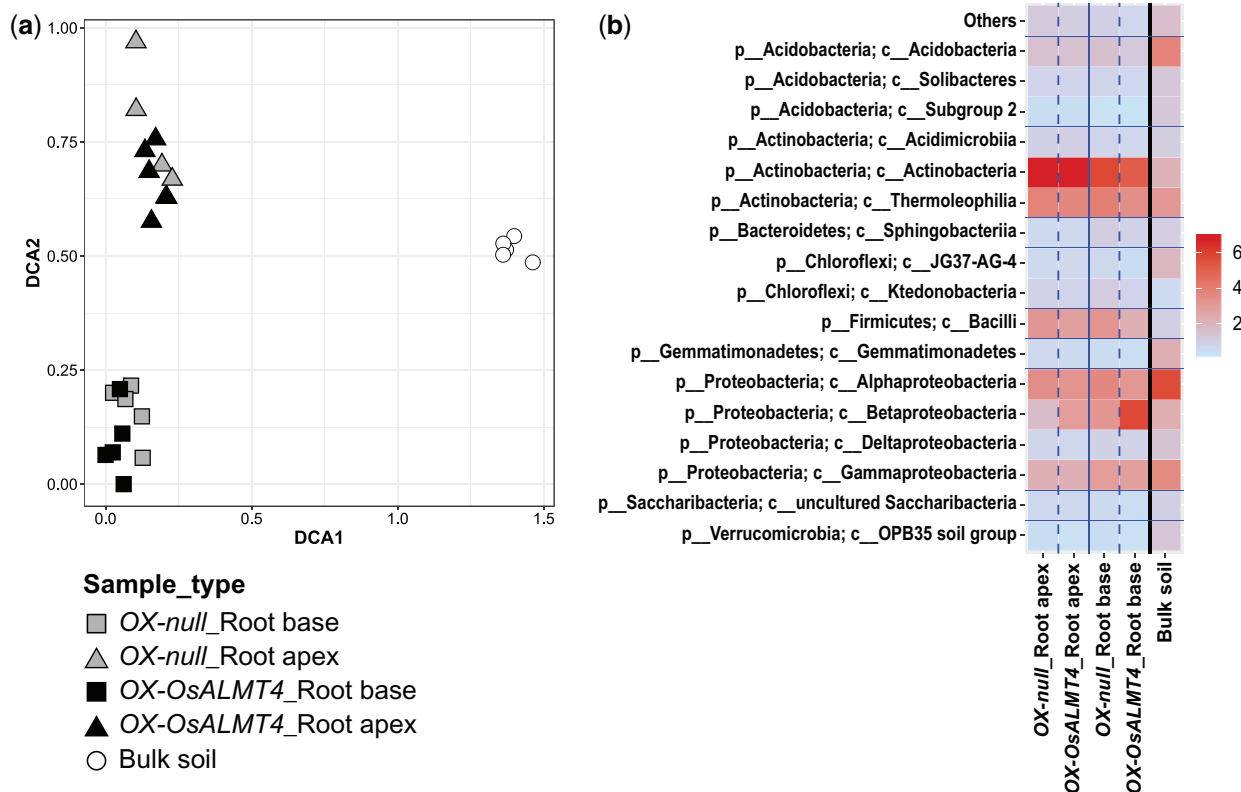


**Figure 2** OsALMT4 activity alters the bacterial microbiome on rice roots. Rice lines *OX-null* and *OX-OsALMT4* were grown in a Yellow Chromosol for 8 d (Experiment II). A, DCA plot showing relationships of the bacterial community structures between the root apices, root bases, and bulk soil samples ( $n = 5$ ). Statistical tests with *mvabund* showed that communities colonizing the root apices and bases were significantly different from each other, and both were significantly different from the bulk soil ( $P < 0.005$ ). Moreover, analysis with *mvabund* showed the communities at the root apices of *OX-OsALMT4* were significantly different from *OX-null* plants ( $P = 0.02$ ), and communities at the root bases of *OX-OsALMT4* were also significantly different from *OX-null* plants ( $P = 0.006$ ). B, A heatmap depicting the relative abundance of bacterial classes in each sample group. Minor bacterial classes ( $< 0.5\%$  in the abundance in any single sample) were compiled into “Others.” Data are means ( $n = 5$ ) and the color scale represents the square root of relative abundance.

Actinobacteria and Ktedonobacteria (Phylum Chloroflexi), showed the reverse pattern, being more abundant on the root apices from the gypsum-amended Ferrosol. Among the 15 OTUs enriched at the root bases of plants grown in the Ferrosol compared with the amended Ferrosol (Figure 5B) were seven Actinobacteria (mostly *Streptomyces*) and three *Peptoclostridium* OTUs (Class Clostridia). Two of these *Peptoclostridium* (OTU875 and OTU2064) were also more abundant at the root apices of plants from the Ferrosol. Lastly, seven OTUs from several Classes were enriched at the root bases of plants grown in the amended Ferrosol compare to the unamended soil (Figure 5B). Details of these OTUs are provided in Supplemental Table S2. For the fungi, 17 OTUs mostly from Classes Eurotiomycetes and Sordariomycetes were more abundant at the root apices from the gypsum-amended Ferrosol (Figure 6A). Nine fungal OTUs differed in abundance at the root bases in the two soils, most being enriched in plants grown in the amended Ferrosol (Figure 6B). A detailed description of these fungal OTUs is provided in Supplemental Table S3.

Since the addition of gypsum to the Ferrosol significantly shifted the bacterial communities in the bulk soil samples,

we needed to determine whether those changes caused the differences in root microbiomes. We conclude that the differences in root microbiomes were not caused by differences in the bulk soil communities for two reasons. First, the magnitude of differences in the bulk soil samples after adding gypsum was much smaller than the differences between the root samples grown in the two soils (Figure 4). Second, the changes that occurred in the OTUs from the bulk soil samples after gypsum addition were not reflected in the root samples of plants grown in those soils. For example, eleven bacterial OTUs from the Chloroflexi were enriched in the bulk soil samples of the Ferrosol relative to the amended Ferrosol (Figure 5C), but no members of this group showed the same preference in the root samples collected from these soils (Figure 5, A and B). Moreover, in the Ferrosol-grown plants, six Clostridia OTUs were enriched on the root apices and three Clostridia OTUs were enriched on the root bases, yet the two bulk soils showed no differences in Clostridia abundance (Figure 5). Similarly, among the fungi, 25 OTUs (mostly Sordariomycetes and Eurotiomycetes) showed significant differences in abundance between the root apices of plants from the Ferrosol and amended

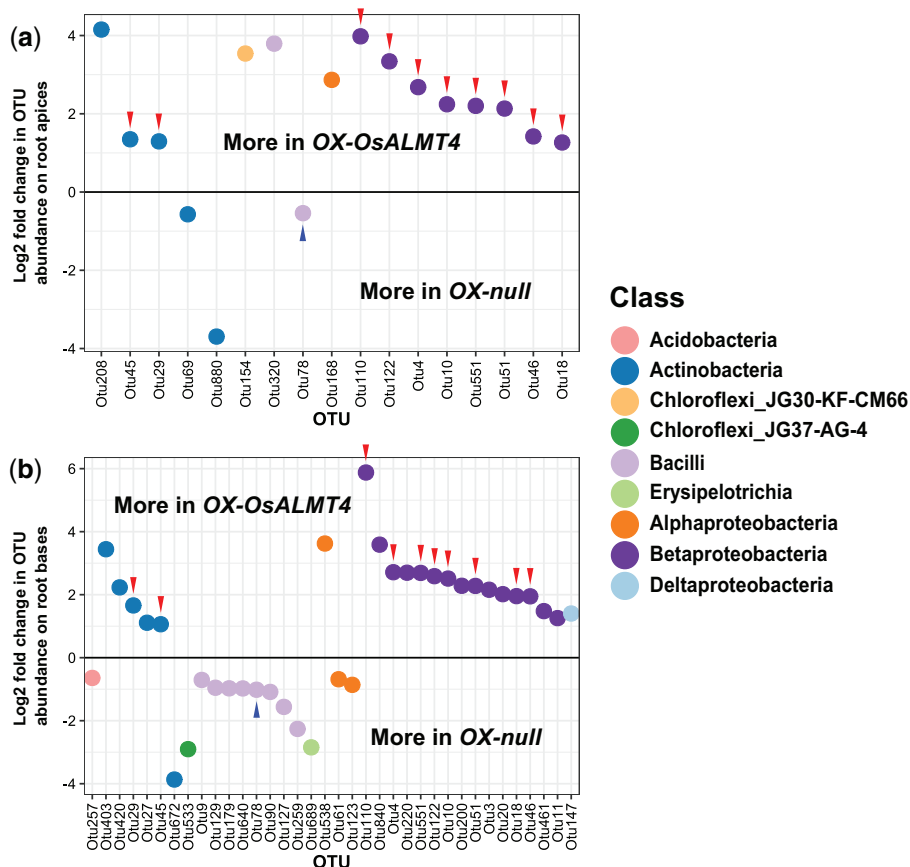


**Figure 3** Bacterial OTUs on rice roots significantly affected by *OsALMT4* activity. Rice lines *OX-null* and *OX-OsALMT4* were grown in a Yellow Chromosol for 8 d (Experiment II). Plots present bacterial OTUs showing significant differences in abundance between the *OX-null* and *OX-OsALMT4* at the (A) root tips and (B) root bases (Wald test  $P < 0.05$ ). Log<sub>2</sub>-fold changes in the OTU abundance between the two sample groups were determined with *DESeq2* ( $n = 5$ ). A and B, The red and blue arrows indicate the OTUs that were more abundant on *OX-OsALMT4* and *OX-null*, respectively, at both the root apices and the root bases.

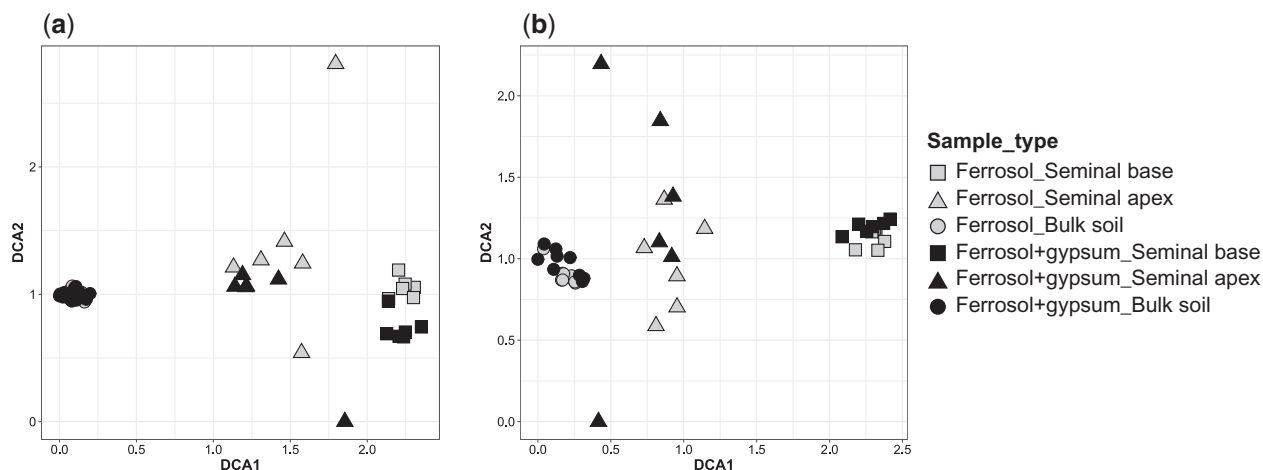


**Figure 4** Effect of *TaALMT1* activity on the microbiome structure along wheat roots. *NIL-null* wheat was grown in the Ferrosol and gypsum-amended Ferrosol for 8 d (Experiment III). DCA plots show the (A) bacterial and (B) fungal community relationships on the seminal root apices, seminal root bases, and the bulk soils in the Ferrosol (*TaALMT1* is active) and the gypsum-amended Ferrosol (*TaALMT1* is not active;  $n = 5-6$ ). The *mvabund* analyses showed the bacterial and fungal communities colonizing the root apices from the Ferrosol were significantly different from those from the amended Ferrosol. Similarly, the communities at the root bases from the Ferrosol were significantly different from the amended Ferrosol ( $P < 0.005$ ). Addition of gypsum to the Ferrosol also caused small but significant shifts in the microbial populations in the bulk soil samples ( $P < 0.005$ ).

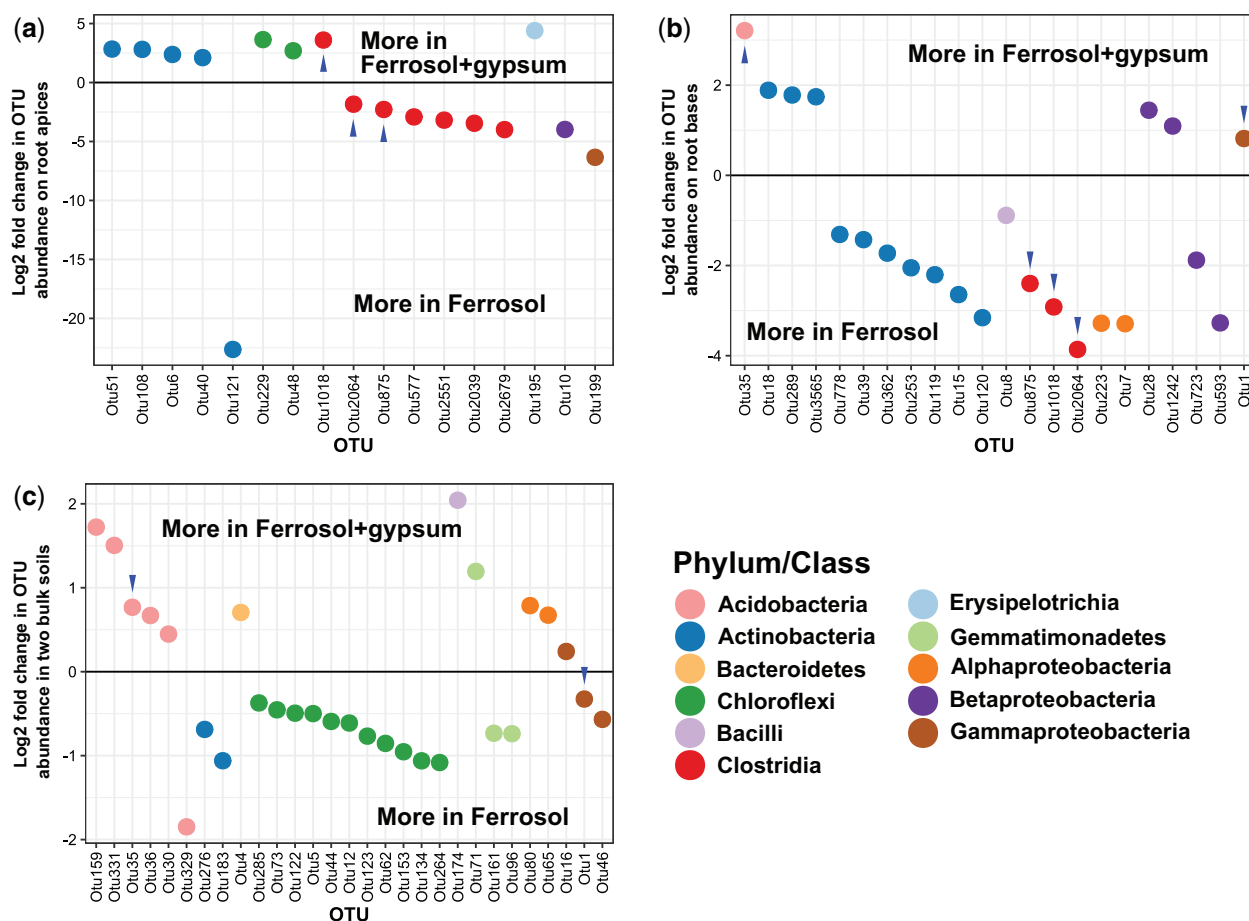


**Figure 5** The effect of TaALMT1 activity on the bacterial microbiome of wheat roots. Plots present the bacterial OTUs that show significant differences (Wald test  $P < 0.05$ ) in abundance between *NIL-null* plants grown in the Ferrosol (TaALMT1 active) or gypsum-amended Ferrosol (TaALMT1 not active) at the (A) seminal root apices and (B) seminal root bases (Experiment III). Also shown in (C) are the bacterial OTUs in the bulk soil samples that are significantly different between the Ferrosol and the gypsum-amended Ferrosol. Log<sub>2</sub>-fold changes in the OTU abundance between the two sample groups were determined with *DESeq2* ( $n = 5-6$ ). A–C, Blue arrows indicate OTUs that appear in more than one plot. The Phylum Firmicutes were subclassified into the Classes Clostridia, Erysipelotrichia, and Bacilli, and the Phylum Proteobacteria was subclassified into the Classes Alphaproteobacteria, Betaproteobacteria, and Gammaproteobacteria.

Ferrosol (Figure 6a). Only two of these (OTU24 and OTU75) showed similar differences between the bulk soils, which again indicates the root assemblages were predominantly influenced by differences in TaALMT1 activity and not by the differences between the two soils (Figure 6c). The results indicate that TaALMT1 activity significantly altered the bacterial and fungal microbiomes on wheat roots and, therefore, the null hypothesis is rejected.

### Effect of TaMATE1B activity on the microbiome of wheat roots, alone, and in combination with TaALMT1

*NIL-null* plants (no citrate release) and *NIL-TaMATE1B* plants (citrate release from the root apices) were grown in a Red Chromosol and the acidic Ferrosol. Since both genotypes have high levels of TaALMT1 expression, they will both release malate and other substrates from their root apices via TaALMT1 when grown in the Ferrosol, but not in the Red Chromosol (Table 1). The null hypotheses tested in this experiment were: (1) citrate release via TaMATE1B does not

affect the root microbiome of plants grown in the Red Chromosol and (2) citrate release does not further alter the root microbiomes of plants grown in the Ferrosol, where TaALMT1 is also active.

Final shoot biomass of *NIL-null* and *NIL-TaMATE1B* plants after 8 and 31 d of growth in the two soils is shown in Supplemental Figure S4. Multivariate analysis (DCA) showed the bacterial and fungal community structures in the bulk soils and on the roots (Supplemental Figure S5). The tight clustering of the bulk soil samples demonstrates that depth in the pots (top, middle, and bottom layers) and time of sampling (8 and 31 d) had little effect on the soil microbial communities. They also highlight that roots had a stronger influence on the bacterial communities than on the fungal communities in these soils (Supplemental Figure S5).

The microbiome communities on different root tissues were first compared to one another by combining data from both genotypes. The DCA plots and *mvabund* pairwise comparisons showed that the bacterial (Supplemental Figure

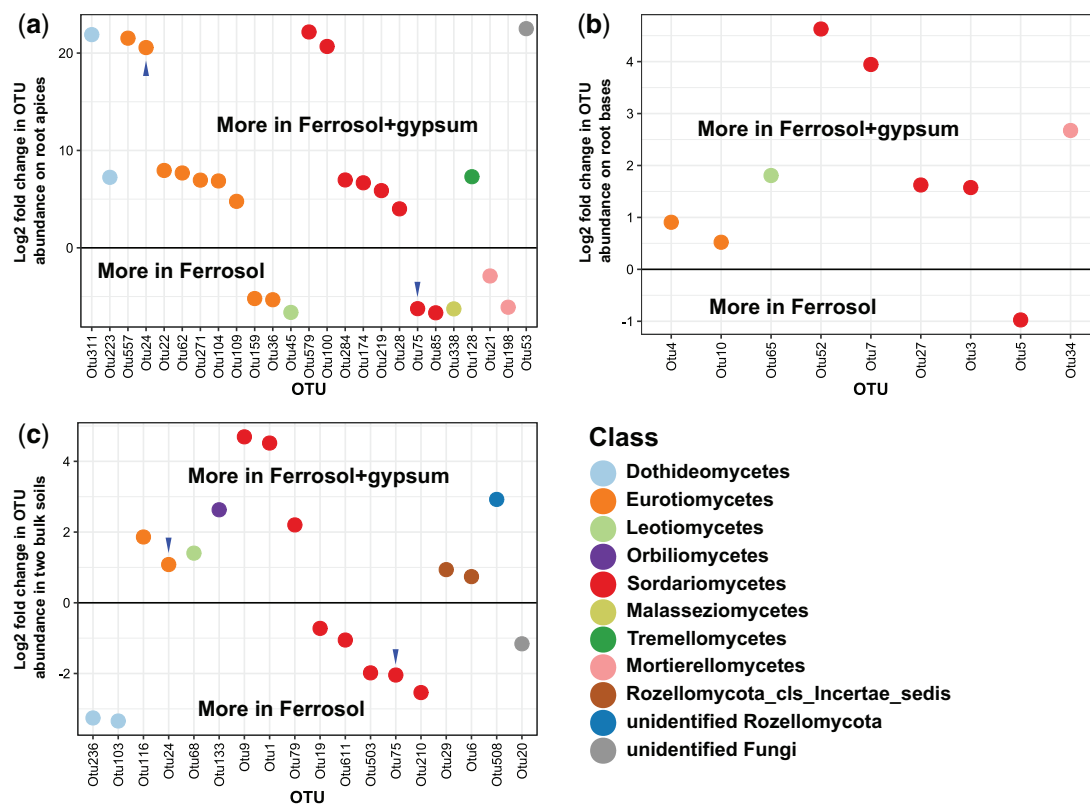


**Figure 6** The effect of TaALMT1 activity on the fungal microbiome of wheat roots. Plots present the fungal OTUs that show significant differences (Wald test  $P < 0.05$ ) in abundance between *NIL-null* plants grown in the Ferrosol (TaALMT1 active) or gypsum-amended Ferrosol (TaALMT1 not active) at the (A) seminal root apices and (B) seminal root bases (Experiment III). Also shown in (C) are the fungal OTUs in the bulk soil samples that are significantly different between the Ferrosol and the gypsum-amended Ferrosol. Log<sub>2</sub>-fold changes in the OTU abundance between the two sample groups were determined with *DESeq2* ( $n = 6$ ). A–C, Blue arrows indicate OTUs that appear in more than one plot.

S6, A and B) and fungal (Figure S6, C and D) communities on seminal root apices, seminal root bases, nodal root apices, and nodal root bases were significantly different from each other in both soils tested (*mvabund*  $P < 0.005$  for all comparisons). The broad patterns that emerged among the bacterial and fungal taxa across the different soils and tissues types are summarized in Supplemental Figures S7 and S8.

We assessed the effect of citrate release on the root microbiome by comparing the communities on *NIL-null* and *NIL-TaMATE1B* roots grown in the Red Chromosol. Microbial community structures on each tissue type were compared between the two genotypes (Supplemental Figure S9) and results summarized in Table 2. For the bacteria, significant differences between the genotypes were detected at the apices of seminal roots, at the bases of seminal roots and at the bases of nodal roots. For the fungal communities, significant differences occurred at the bases of seminal roots only, but the difference at the apices of seminal roots was almost significant (*mvabund*  $P = 0.055$ ; Table 2). The bacterial OTUs showing significant differences in abundance between *NIL-null* and *NIL-TaMATE1B* are presented in Figure 7 and Supplemental Table S4, and the fungal OTUs showing significant differences in abundance are shown in Figure 8 and Supplemental Table S5. Many bacterial OTUs showed a clear preference for one genotype over another in the Red

Chromosol. For example, eight Clostridia OTUs (best close match *Peptoclostridium*) were preferentially enriched at the seminal root apices of *NIL-TaMATE1B* (Figure 7A), 11 Betaproteobacteria OTUs (mostly from Families Oxalobacteraceae, Burkholderiaceae, and Comamonadaceae) were enriched at the nodal root apices of *NIL-TaMATE1B* (Figure 7B) and six Actinobacteria OTUs (including *Streptomyces* and *Streptacidiphilus*) were enriched at the seminal root bases of *NIL-null* plants (Figure 7C). Two Bacilli (OTU8 and 74) were more abundant on *NIL-null* plants at the bases of both root types and, interestingly, one OTU from the Gammaproteobacteria (OTU1, uncultured *Rhodanobacter*) was enriched at the apices of seminal and nodal roots from *NIL-TaMATE1B* but enriched at the root bases of *NIL-null* (Figure 7). Several fungal OTUs also showed differences in abundance between the *NIL-null* and *NIL-TaMATE1B*, with one unidentified Basidiomycota (OTU141) being significantly more abundant at the bases of the seminal and nodal roots of *NIL-null* plants (Figure 8, C and D).

Finally, we assessed whether citrate release via TaMATE1B could alter the root microbiome when TaALMT1 is also active. This was done by comparing the microbial population from *NIL-null* and *NIL-TaMATE1B* plant roots grown in the Ferrosol (Table 1). Microbial community structures of the two genotypes on each tissue type were characterized with



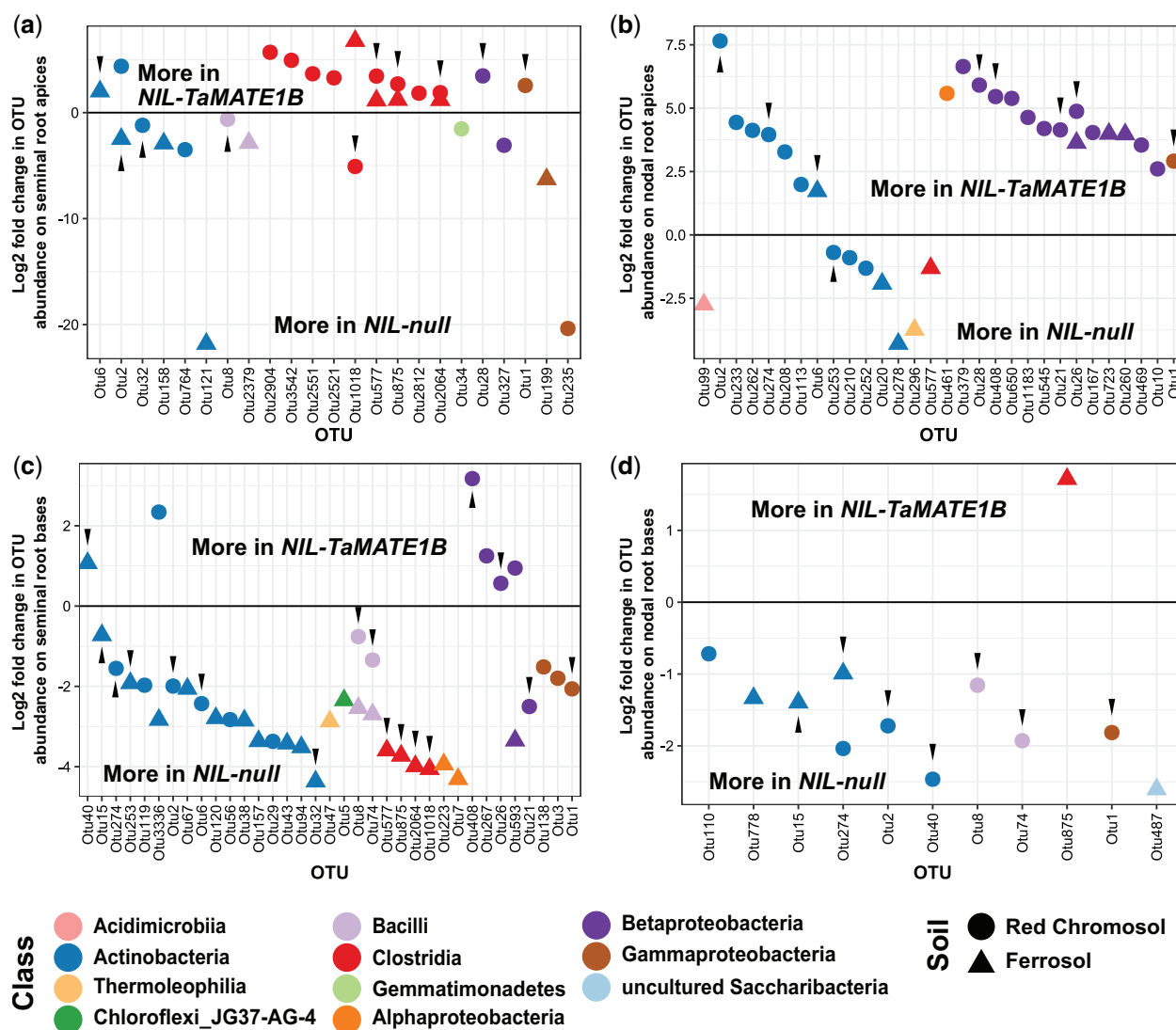


**Figure 7** Effect of TaMATE1B activity on the bacterial microbiome of wheat roots with and without TaALMT1 activity. Wheat plants *NIL-null* and *NIL-TaMATE1B* were grown in a Red Chromosol (filled circle; TaALMT1 not active) or Ferrosol (filled triangle; TaALMT1 active; Experiment IV). Plots present bacterial OTUs showing significant differences in abundance between *NIL-null* and *NIL-TaMATE1B* on the (A) seminal root apices, (B) nodal root apices, (C) seminal root bases, and (D) nodal root bases (Wald test  $P < 0.05$ ). Log<sub>2</sub>-fold changes in the OTU abundance between the two sample groups were determined with *DESeq2* ( $n = 6$ ). A–D, Black arrows indicate OTUs that appear in more than one plot.

DCA (Supplemental Figure S10) and results from the *mva-bund* analyses are summarized in Table 2. Pairwise comparisons of the bacterial communities showed significant differences between *NIL-null* and *NIL-TaMATE1B* at the base of seminal roots and at the apices of nodal roots. For the fungi, significant differences between *NIL-null* and *NIL-TaMATE1B* were detected only at the base of nodal roots (Table 2).

Relatively, few bacterial groups showed differences in abundance on *NIL-TaMATE1B* roots (malate and citrate release) compared with *NIL-null* roots (malate release only) in the Ferrosol. A member of the Actinobacteria (OTU6) was more abundant at the root apices of both seminal and nodal roots of *NIL-TaMATE1B*, and this was joined by four Clostridia (OTU1018, 577, 875, and 2064) at the seminal root apices (Figure 7, A and B). Three Betaproteobacteria

(OTU26, 723, and 260) were more abundant at the apices of nodal roots of *NIL-TaMATE1B* (Figure 7B). Among other shifts in bacterial abundance detected only in the Ferrosol were four Clostridia, two Alphaproteobacteria (uncultured *Sphingomonas*), a Thermoleophilia (uncultured YNPFFP1) and a Chloroflexi\_JG37-AG-4 enriched at the seminal root bases of *NIL-null* plants (Figure 7C), and a single uncultured Saccharibacteria (OTU 487) which were more abundant on the nodal root bases of *NIL-null* plants (Figure 7D). Several fungal groups showed shifts in abundance only in the Ferrosol-grown plants, including a Mortierellomycetes (OTU289) and a Rozellomycota (OTU6), which were enriched at the seminal root apices of *NIL-TaMATE1B* (Figure 8A), a Eurotiomycetes (OTU62), and a Leotiomyces (OTU117) which were enriched at the nodal root apices of *NIL-null* (Figure 8B), and three Orbiliomycetes OTUs that

**Table 2** Effect of TaMATE1B activity on the microbiome of wheat roots with and without TaALMT1 activity

Root Tissues	Effect of TaMATE1B Activity on the Root Microbiome NIL-Null versus NIL-TaMATE1B ( <i>mvabund</i> P-values)			
	Red Chromosol (TaALMT1 not active)		Ferrosol (TaALMT1 active)	
	Bacteria	Fungi	Bacteria	Fungi
Seminal Apices	0.001*	0.055*	0.169	0.385
Seminal Bases	0.003*	0.040*	0.002*	0.710
Nodal Apices	0.094	0.260	0.003*	0.685
Nodal Bases	0.012*	0.145	0.113	0.010*

Summary of tests comparing the effect of TaMATE1B activity on the root microbiomes grown in the Red Chromosol and Ferrosol (Experiment IV, Table 1). TaALMT1 is active in the Ferrosol but not in the Red Chromosol. Differences in the microbial community structures between the two genotypes (*NIL-null* and *NIL-TaMATE1B*) in each root tissue were assessed with a multivariate GLM and a negative binomial distribution using the *mvabund* package. Shown are the *mvabund* P-values on the bacterial and fungal microbiomes from different root tissues and two soils. Significant differences ( $P < 0.05$ ) are shown by an asterisk, with the exception of fungi in the seminal root apices in the Red Chromosol where  $P = 0.055$ .

were enriched at the nodal root bases of *NIL-TaMATE1B* (Figure 8D). Details of these bacterial and fungal OTUs can be found in Supplemental Tables S4 and S5, respectively.

Changes that were similar in the Red Chromosol and the Ferrosol included enrichment of Clostridia OTUs (best close match *Peptoclostridium*) on the seminal root apices of *NIL-TaMATE1B* (Figure 7A), an enrichment of Betaproteobacteria (Families Oxalobacteraceae, Burkholderiaceae, Pseudonocardiaceae, and Comamonadaceae) on the nodal root apices of *NIL-TaMATE1B* (Figure 7B) and the enrichment of Actinobacteria (including *Streptomyces* and *Streptacidiphilus*) on the seminal root bases of *NIL-null* plants (Figure 7C).

OTUs that displayed similar shifts across both seminal and nodal root types included the bacterial OTU1 (*Rhodanobacter*), OTU2 (*Streptacidiphilus*), OTU6 (*Amycolatopsis*), and OTU28 (*Burkholderia/Paraburkholderia*), which were enriched at the apices of both seminal and nodal roots of *NIL-TaMATE1B* (Figure 7, A and B), as well as OTU1 (*Rhodanobacter*), OTU2 (*Streptacidiphilus*), OTU8 (*Bacillus*), OTU15 (*Streptomyces*), OTU74 (*Sporosarcina*), and OTU274 (*Streptacidiphilus*), which were consistently more abundant in *NIL-null* plants at the bases of both root types (Figure 7, C and D). Seven bacterial OTUs (OTU8, 26, 74, 274, 577, 875, and 2064) displayed the same genotype-specific enrichment in both soils, while four OTUs (OTU2, 593, 1018, and 3336) swapped their genotype preference in the two soils (Figure 7; Supplemental Table S4). Among the fungi, the unidentified Ascomycota and Basidiomycota, and most Eurotiomycetes OTUs were more abundant in *NIL-null* plants than *NIL-TaMATE1B* plants. A Chaetomiaceae (OTU19, Class Sordariomycetes) and an unidentified Clavicipitaceae (OTU85, Class Sordariomycetes) were more abundant on the seminal root apices of *NIL-null* plants but more abundant on the seminal root bases of *NIL-TaMATE1B* plants (Figure 8; Supplemental Table S5). The null hypotheses are rejected because TaMATE1B activity, alone and in combination with

TaALMT1 activity, was able to alter the microbiome at some regions of the root system.

## Discussion

This study investigated whether the root microbiome can be manipulated in a consistent manner by modifying the expression of membrane transporters and their exudates from roots. The aim was not to generate a beneficial microbiome per se, although that is the ultimate goal of this work and remains a major challenge. Instead, we aimed, first, to demonstrate that varying transporter activity provides a means of changing the root microbiome in a consistent manner and, second, to assess how those changes differ throughout the root system. We demonstrated that by varying the activity of OsALMT4 in rice (*O. sativa* L.) and the activity of TaALMT1 and TaMATE1B in wheat (*T. aestivum* L.), we could modify the root exudates and significantly alter the microbial communities at the root apices and the root bases. Moreover, we showed that these changes differed between different root types.

We identified specific bacterial and fungal OTUs that showed consistent preferences for plants releasing simple organic anions. For example, a total of 14 bacterial OTUs (largely *Burkholderia/Paraburkholderia*, *Leifsonia*, and *Pseudarthrobacter*) were significantly more abundant at the root apices of the rice line releasing malate than from the control line (Figure 3A; Supplemental Table S1). In wheat, bacterial OTUs closely matching *Peptoclostridium*, *Arthrobacter*, *Massilia*, and *Alkanindiges* were more abundant at the root apices when TaALMT1 was activated and malate and GABA were released (Figure 5A; Supplemental Table S2). Similarly, OTUs from the *Streptacidiphilus*, *Amycolatopsis*, and *Burkholderia/Paraburkholderia* were more abundant on the apices of seminal and nodal roots of the citrate-releasing wheat line *NIL-TaMATE1B*, whereas *Rhodanobacter*, *Bacillus*, *Streptomyces*, and *Sporosarcina* were consistently more abundant at the bases of the seminal and nodal roots of *NIL-null* plants that do not release citrate (Figure 7; Supplemental Table S4). Among the fungi, OTUs from the *Ophiosphaerella* (OTU23) and *Cladosporium* (OTU48) genera were more abundant on wheat roots releasing citrate (Figure 8; Supplemental Table S5).

The finding that *Peptoclostridium* (Clostridia) and *Massilia* (Betaproteobacteria) were enriched on root apices of *NIL-TaMATE1B* wheat in two different soils (Figure 7, A and B; Supplemental Table S4), as well as on the roots of wheat when TaALMT1 was activated (*Peptoclostridium* OTU875 and 2064; Figure 5, A and B; Supplemental Table S2), suggests these groups benefit from the substrates released via TaMATE1B (citrate) and TaALMT1 (malate, GABA, and smaller amounts of other organic anions). This is consistent with other reports demonstrating Clostridia species produce citrate lyase that enables them to catabolize citrate as a sole carbon source (Walther et al., 1977; Antranikian et al., 1984; Quentmeier and Antranikian, 1985). Interestingly, Clostridia were only enriched on the seminal root apices of *NIL-*

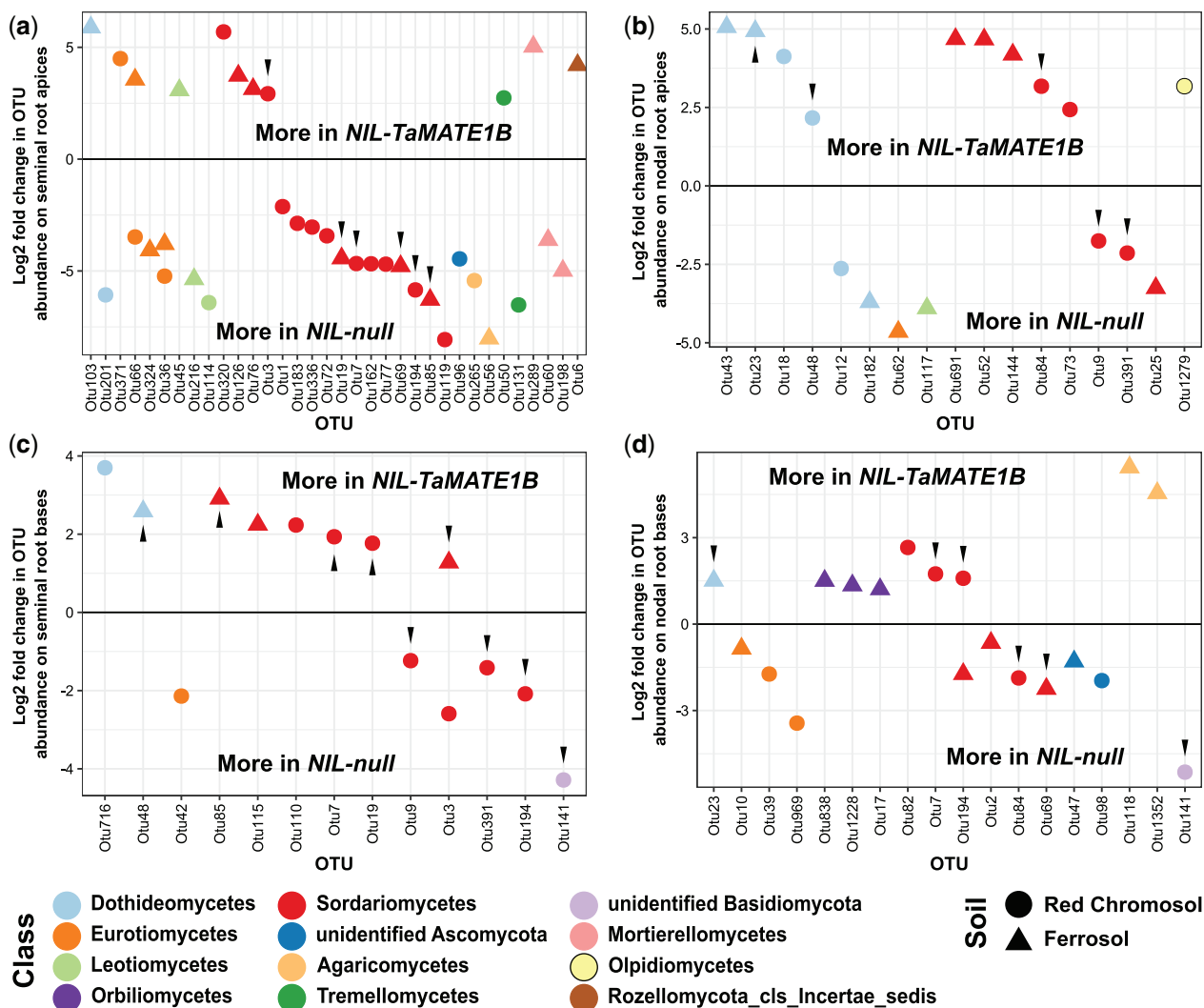


**Figure 8** Effect of TaMATE1B activity on the fungal microbiome of wheat roots with and without TaALMT1 activity. Wheat plants *NIL-null* and *NIL-TaMATE1B* were grown in a Red Chromosol (filled circle; TaALMT1 not active) or Ferrosol (filled triangle; TaALMT1 active; Experiment IV). Plots present fungal OTUs showing significant differences in abundance between *NIL-null* and *NIL-TaMATE1B* on the (A) seminal root apices, (B) nodal root apices, (C) seminal root bases, and (D) nodal root bases (Wald test  $P < 0.05$ ) were elucidated with *DESeq2*. Log<sub>2</sub>-fold changes in the OTU abundance between the two sample groups were determined with *DESeq2* ( $n = 6$ ). A–D, Black arrows indicate OTUs that appear in more than one plot.

*TaMATE1B* wheat and not on the nodal root apices (Figure 7, A and B), despite them releasing similar amounts of citrate (Figure 1). This indicates that other factors also influence the structure of these microbial communities. The nodal root apices of *NIL-TaMATE1B* instead harbored more Betaproteobacteria (Families Burkholderiaceae, Oxalobacteraceae, and Comamonadaceae) than those of *NIL-Null* (Figure 7B), and OTUs from these same Families were also enriched all along the roots of the malate-releasing rice *OX-OsALMT4* (Figure 3; Supplemental Table S1). We conclude that these groups also benefited from the substrates released via the transporters, which supports previous findings that members of these families are able to utilize organic acids as a sole carbon source (Willems et al., 1991; Baldani et al., 2014). The Order Burkholderiales (Class

Betaproteobacteria) are also abundant on the cluster roots of white lupin (*Lupinus albus* L.), which release large amounts of citrate and malate and other substrates to improve phosphate availability in the soil (Weisskopf et al., 2011). This information linking root exudates with the proliferation of specific microbial groups could be used to manipulate root microbiomes.

GABA is a nonprotein amino acid found in most prokaryotic and eukaryotic organisms. Not only is it a substrate of the ALMTs examined in heterologous expression systems so far (Ramesh et al., 2015), but it can also interact with malate to regulate TaALMT1 activity (Ramesh et al., 2018). Many soil microorganisms produce GABA and it is often detected in root exudates. GABA has been predicted to have a role in quorum sensing and in plant–microbe interactions (Chevrot

et al., 2006), and appears to be essential for the culture of some microorganisms (Strandwitz et al., 2019). Whether the release of GABA via ALMTs influences the microbiomes developing on rice and wheat roots needs to be determined. Certainly, OTUs from the Family Peptostreptococcaceae (Class Clostridia) were only enriched on wheat roots when malate and GABA were exuded (Figures 5, A, B, and 7, A). It will be intriguing to determine whether GABA is essential for the proliferation of some beneficial soil microorganisms. If it is, then the manipulation of ALMT transporters could provide a means of attracting those species to the roots.

Notwithstanding the clear patterns described above for some OTUs, the influence of transporter activity on the root microbiome remained relatively small compared with the influence of tissue type and soil. Root type (seminal or nodal root), the location along the root (apex or base), and soil type had a larger influence on shaping the bacterial and fungal populations on the roots than the expression of the transporters and their exudates (Figures 2 and 4; Supplemental Figures S5–S8). Other changes to the microbiome were more difficult to interpret. For instance, the communities that developed on seminal roots of wheat were not always observed on the nodal roots (e.g. Clostridia), even though TaALMT1 and TaMATE1B functioned similarly on both root types and the root apices of these roots had similar ages (Figure 1; Kawasaki et al., 2018). It is possible that the full catalog of substrates released from these different root types is incomplete. Alternatively, root types might affect microbial growth in other ways, such as through rhizosphere pH, redox status, or even cell wall composition.

Microbiomes on the root apices were consistently distinct from those on the root bases, which agrees with previous reports (Dennis et al., 2010; Kawasaki et al., 2021; R uger et al., 2021). Since exudation via the TaMATE1B and TaALMT1 is largely restricted to the root apices, it might have been expected that they would drive greater changes to the microbiome composition compared with the soil communities and those on the root bases. This was not the case. Instead, results in Figure 4 show that overall community structure of microbiomes on the root bases is more dissimilar to the bulk soil than the communities on the root apices. Previous reports discussing this same pattern concluded that root growth allowed too little time for the microbiome at the root apices to fully respond to the exudates (Dennis et al., 2009). Mature root tissues have a different range of rhizodeposits and more time to affect the microbiome. Nevertheless, some OTUs showed a similar enrichment at the root apices and the root bases. For example, in rice, eight OTUs from the *Burkholderia/Paraburkholderia* (Betaproteobacteria) and others from *Leifsonia* and *Pseudarthrobacter* (Actinobacteria) were more abundant at the root apices and the root bases of OX-OsALMT4 compared with the OX-null (Figure 3). Perhaps, these OTUs began to proliferate as the roots first began to emerge and were able to persist and maintain the colonization as the root grew on.

The spatial variation of the root microbiome presents us with additional challenges, especially if we need to target specific regions of the root to combat diseases or improve nutrition. Although transporters manipulated in this study altered the microbial communities at the root apices and the root bases, the greatest direct influence of the exudates on microbiome composition will still be at the site of exudation. Once the exudates are released to the soil, they will be rapidly assimilated by microorganisms and involved in metabolic pathways and population cycles that are beyond plant control. The carbon pools and microbial communities away from root apices are less likely to be determined by the original exudates (Dennis et al., 2010). The role of exudates in structuring the root and rhizosphere communities needs to be considered in the context of the carbon pools already in the soil as well as the resident microbial communities there. This will be important when attempting to manipulate the root microbiome on particular root tissues or for promoting the stability of inoculants.

## Conclusions

Sustainable farming systems attempt to balance inputs with crop requirements (Padilla et al., 2018; Wang et al., 2019) and a necessary step toward achieving this goal requires us to fully exploit the genetic potential of crops to resist biotic and abiotic stresses. This extends to the rhizosphere and the microbial interactions occurring at the plant–soil interface that can benefit plant growth (Pii et al., 2015). This study demonstrated that simple organic compounds in the root exudates can shift the root microbiome composition on major crop species, and that transgenic and nontransgenic approaches can achieve this. We also demonstrate that the spatial variation of the microbiome within the root system is high and that the root type and location on roots had a greater effect on the microbiome structure than the exudates. Finally, we identified specific bacterial and fungal OTUs that were robustly linked with the activity of transporters and their exudates (or lack thereof) on different root types and across different soils. Future investigations need to determine the key components of a beneficial microbiome and the substrates and conditions that will encourage its development. Once these are known, the transporters likely to mimic those conditions can be identified and manipulated.

## Materials and methods

### Plant materials

This study used transgenic lines of rice (*O. sativa* L.; cv Nipponbare) that differs in malate release and a pair of NILs of wheat (*T. aestivum* L.) that differs in citrate release from the roots. The transgenic rice was generated by overexpressing *OsALMT4* using the maize *ubiquitin* promoter. The resulting OX-OsALMT4 (homozygous T4) line showed a constitutive release of malate from the root apices (of  $\sim 0.5$  nmol apex<sup>-1</sup> h<sup>-1</sup>), while the null-segregant sister line



(*OX-null*) showed no malate release (Liu et al., 2017). When expressed in heterologous systems, OsALMT4 was also permeable to GABA (Ramesh et al., 2015; NB: OsALMT4 was designated as OsALMT5 in that study).

The wheat NILs varying in citrate release were selected from a BC<sub>9</sub>F<sub>4</sub> population (Han et al., 2016) where cv Carazinho was the donor of the mutant *TaMATE1B* allele that confers a constitutive release of citrate from seminal roots (~100 pmol apex<sup>-1</sup> h<sup>-1</sup>; Ryan et al., 2009b; Tovkach et al., 2013). These NILs were named *NIL-TaMATE1B* (citrate release) and *NIL-null* (no citrate release). Both NILs possess the Type V allele for *TaALMT1* (Sasaki et al., 2006) which, when activated by the Al<sup>3+</sup> in acidic soils, will release malate (~1 nmol apex<sup>-1</sup> h<sup>-1</sup>) from the apices of axile and lateral roots of the seminal and nodal root systems (Sasaki et al., 2004; Kawasaki et al., 2018). *TaALMT1* is also permeable to GABA and other organic anions (Piñeros et al., 2008; Sharma et al., 2016; Ramesh et al., 2018).

The NILs of wheat ET8 and ES8 (Ryan et al., 1995) were used in preliminary growth experiments to test whether the soils contained toxic levels of Al<sup>3+</sup>. ET8 (Al<sup>3+</sup>-tolerant) and ES8 (Al<sup>3+</sup>-sensitive) vary in tolerance because they possess different alleles of *TaALMT1* (Sasaki et al., 2006; Raman et al., 2008). In Al<sup>3+</sup>-toxic soils, the root growth of ET8 is greater than ES8 because the release of malate protects the growing root apices. In soils that do not contain toxic Al<sup>3+</sup>, their growth is similar (Supplemental Figure S2).

### Citrate efflux and *TaMATE1B* expression on different root types of wheat

Table 1 summarizes the aims and designs of all experiments reported here. Experiment I grew the wheat NILs (*NIL-null* and *NIL-TaMATE1B*) in a sterile hydroponic system (five replicate plants per genotype) as described previously (Kawasaki et al., 2018) for 3 weeks, by which time they had developed about five seminal, eight nodal, and hundreds of lateral roots. Root exudates were collected from different parts of the root system as described previously (Kawasaki et al., 2018), and citrate in the exudates was quantified with Abcam Citrate Assay Kit (Abcam, VIC, Australia) by fluorescence detection using a TECAN Infinite M200 PRO microplate reader.

RNA was extracted from the wheat root apices using the RNeasy Plant Mini Kit (QIAGEN, VIC, Australia) according to the manufacturer's protocol, which included a DNase step. cDNA synthesis and amplification and quantification of *TaMATE1* transcripts are described previously using glyceraldehyde 3-phosphate dehydrogenase and  $\alpha$ -tubulin as reference genes (Ryan et al., 2009b; Tovkach et al., 2013).

### Description of soils

Soils were collected from the 10–20 cm layer at three locations and soil pH was measured in 0.01 M CaCl<sub>2</sub> solution (1:5 w/v soil:solution). The Yellow Chromosol (pH 4.3) was collected from a sheep grazing paddock at the CSIRO Ginninderra Experimental Station, Australia (35°10'30"S 149°02'33.4"E). Although acidic, the Yellow Chromosol did

not contain toxic concentrations of Al<sup>3+</sup>, as confirmed by preliminary growth experiments with ET8 and ES8 (Supplemental Figure S2). The Ferrosol (pH 4.3) was collected from a cattle grazing paddock near Robertson, Australia (34°37'37.9"S 150°28'53.7"E). It contained toxic levels of Al<sup>3+</sup> as confirmed in preliminary experiments (Supplemental Figure S2). It was also highly P-fixing and therefore amended with KH<sub>2</sub>PO<sub>4</sub> (250 mg P kg<sup>-1</sup> dry soil). In Experiment III described below, the Ferrosol was further amended with gypsum (5 g CaSO<sub>4</sub> kg<sup>-1</sup> dry soil) to reduce the concentration of toxic Al<sup>3+</sup> cations without changing pH (Supplemental Figure S2). The Red Chromosol (pH 5.9) was collected from a cereal cropping paddock near Young, Australia (34°19'29.7"S 148°14'42.8"E). All soils were air dried, sieved through 5 mm mesh, and stored at room temperature. Prior to use, deionized water was added to adjust the soil moisture to 80% field capacity for the Yellow Chromosol, 90% for the Ferrosol, and 44% for the Red Chromosol. The soil was packed in short polyvinylchloride (PVC) tubes (9 cm diameter × 20 cm) for the 8 d growth periods and tall PVC tubes (10 cm diameter × 50 cm) for the 31 d growth periods. Tubes were lined with plastic and soil packed at the density of approximately 1 g cm<sup>-3</sup> for Ferrosol and Yellow Chromosol, and 1.4 g cm<sup>-3</sup> for the Red Chromosol.

### Soil experiments

All seeds were surface sterilized with bleach, stratified at 4°C for 2 d, and germinated at room temperature for 3 d. Germinated seedlings were transplanted into the PVC tubes (three wheat seedlings per tube and 10 rice seedlings per tube), covered with plastic pellets to prevent excessive moisture loss, and tubes weighed. The experiments were conducted in a growth cabinet or in a glasshouse with natural light for periods of 8 or 31 d as described below.

Experiment II grew transgenic lines of rice in a Yellow Chromosol to examine the effect of OsALMT4 activity on the root microbiome (Table 1). Five replicate tubes per genotype were placed in a growth cabinet (Conviron, Canada) for 8 d with a 16-h d/8-h night cycle (24°C/20°C) and 600 μmol photon m<sup>-2</sup> s<sup>-1</sup>.

Experiment III used the *NIL-null* wheat line (no citrate release) to examine the effect of *TaALMT1* activity on the root microbiome (Table 1). Plants were grown in a glasshouse for 8 d in the PVC tubes (six replicate tubes per treatment) containing either the Ferrosol (toxic concentrations of Al<sup>3+</sup>) or the same Ferrosol amended with gypsum to reduce the concentration of Al<sup>3+</sup> without changing soil pH. The *TaALMT1* channel will be activated by the Al<sup>3+</sup> cations in the Ferrosol to release malate and GABA. *TaALMT1* will not be activated in the gypsum-amended Ferrosol because the concentration of Al<sup>3+</sup> is too low (Supplemental Figure S2).

Experiment IV examined the effect of *TaMATE1B* activity alone, and in combination with *TaALMT1* activity, on the root microbiome of wheat (Table 1). The *NIL-null* (no citrate release) and *NIL-TaMATE1B* (constitutive citrate release)



wheat lines were grown in the Red Chromosol and a Ferrosol in a glasshouse. The effect of TaMATE1B activity alone (citrate release) on the root microbiome could be tested by comparing the plants grown in the Red Chromosol. The effect of TaMATE1B activity in combination with TaALMT1 activity (malate and GABA release) on the root microbiome could be tested by comparing these lines in the Ferrosol. Two sets of plants were prepared, and seminal root samples were collected from plants after 8 d (from the first set of pots) and nodal root samples were collected after 31 d (from the second set of pots). Six replicate PVC tubes were prepared for each treatment (i.e. two genotypes  $\times$  two soils  $\times$  two growth periods).

Plants were watered daily to the initial weight with deionized water and the tubes were spatially randomized every 2 d. Replicated tubes without plants were also prepared to sample the bulk soil microbiomes at the same time.

### Sampling of root tissues

Rice seedlings grow a single seminal root and then nodal or adventitious roots emerge soon after (Morita and Abe, 1994). Therefore, most of the roots sampled in rice were nodal roots. Wheat initially grows about five seminal roots from the grain and these were sampled after 8 d. Nodal roots in wheat, which emerge 10–14 d later from the crown, were sampled after 31 d from different plants. The plants were removed from the tubes and soil was washed off the roots with tap water. The root microbiome analyzed in this study, therefore, included the organisms colonizing the outer surface of roots after washing, as well as endophytes. Each root was excised from the base of the shoot, and detangled in a shallow tray containing sterile 0.2 mM CaCl<sub>2</sub> solution. The root apices and root bases of the seminal and nodal roots were sampled, rinsed in sterile 0.2 mM CaCl<sub>2</sub>, and stored at  $-80^{\circ}\text{C}$  for DNA extraction. Root apices were defined as the terminal 1 cm of root, and the root bases represented the 2 cm region between 1 and 3 cm from the root base, including any laterals. From each PVC tube, 10–15 root apices and 5–6 root bases were collected and pooled to make a single sample. Bulk soil samples were taken from the middle layer of unplanted tubes in Experiments II and III. Bulk soil samples were also collected from the top (1 cm from surface), middle, and bottom (1 cm from base) of the unplanted PVC tubes in Experiment IV.

### Microbial community analysis

Root samples were lyophilized and then homogenized. DNA was isolated from soil and homogenized root samples using a DNeasy PowerSoil Kit (QIAGEN) according to the kit guidelines.

Bacterial and fungal community sequencing was carried out as described previously (Kawasaki et al. 2021). Bacterial 16S ribosomal RNA (rRNA) genes were amplified using 799F (AACMGGATTAGATACCCCKG) and 1391R (GACGGGCGGTGWGTRCA) primers (Beckers et al., 2016), and a peptide nucleic acid (PNA) clamp TaMtPNA1-F (GCCCCGCTCCGAAACA) was added in the polymerase chain reaction (PCR) to reduce the co-

amplification of the host mitochondrial 18S rRNA gene (Kawasaki et al., 2021; Kawasaki and Ryan, 2021). For wheat root samples, 10  $\mu\text{M}$  PNA was added to the PCR, and the PCR products were separated on 1.5% agarose gels and the bacterial bands ( $\sim 700$  bp) excised. For rice root samples, it was not possible to separate the products on a gel since the rice mitochondrial amplicon is similar in size to the bacterial 16S amplicon; therefore, 20  $\mu\text{M}$  PNA was used to minimize the amplification of rice DNA. Fungal internal transcribed spacer (ITS) was amplified with a semi-nested PCR approach to avoid co-amplification of plant-derived sequences. First round PCR was performed with ITS1F\_KYO1 (CTHGGTCATTTAGAGGAATAA; Toju et al., 2012) and ITS4-R (TCCTCCGCTTATTGATATGC; White et al., 1990), and the second round PCR was performed with gITS7-F (GTGARTCATCGARTCTTTG; Ihrmark et al., 2012) and ITS4-R. The bacterial 16S primers and the fungal ITS primers used for the final amplification (gITS7-F and ITS4-R) had Illumina overhang adapters on the 5'-ends for compatibility with Nextera XT indices. Samples were sequenced on an Illumina MiSeq at The University of Queensland's Institute for Molecular Biosciences (UQ, IMB) using 30% PhiX Control version 3 (Illumina, San Diego, CA, USA) and a MiSeq Reagent Kit version 3 (600 cycles; Illumina).

A modified UPARSE pipeline (Edgar, 2013) was used to analyze both datasets using the forward reads. Primer sequences were removed from the 16S amplicons and trimmed to 250 bp. For ITS sequences, ITSx (version 1.0.11; Bengtsson-Palme et al., 2013) was used to identify and extract ITS2 sequences. After removal of chimeric sequences, USEARCH (version 10.0.240; Edgar, 2010) was used to filter and cluster 16S and ITS sequences into OTUs and generate tables. Taxonomy was assigned to the bacterial and fungal OTU with SILVA SSU (version 128; Quast et al., 2013) and UNITE (version 7.2-2017.10.10; Nilsson et al., 2019) databases, respectively, using BLASTN (version 2.3.0+; Zhang et al., 2000) within QIIME 2 (Bolyen et al., 2019). Nonbacterial OTUs were removed using BIOM tool suite (McDonald et al., 2012). From each Experiment, equal numbers of valid sequences (minimum library size) were rarefied and the OTU tables were used for subsequent statistical analyses.

### Statistical analyses

Statistical analyses were performed in R version 3.5.3 environment (R Core Team, 2019). Hellinger transformation was applied to the OTU tables (Legendre and Gallagher, 2001) and differences in the microbial community composition associated with each sample were visualized after DCA using *vegan* package (Oksanen et al., 2019). Differences in the microbial community structures between the sample groups were assessed with multivariate GLMs using a negative binomial distribution, as implemented in the *mvabund* package (Wang et al., 2012). Significant differences in OTU abundance between two sample groups were identified with the *DESeq2* package (Love et al., 2014) by converting the data with the *phyloseq* package (McMurdie and Holmes, 2013) as described previously (McMurdie and Holmes, 2014).

Negative binomial GLMs were fitted for each OTU, and the logarithmic fold changes in the OTU abundance between the two groups were calculated. Significance was tested using the Wald test with a threshold of  $P < 0.05$ .

### Accession numbers

All sequences from this study have been deposited in the Sequence Read Archive under BioProject accession number PRJNA735611.

### Supplemental data

The following materials are available in the online version of this article.

**Supplemental Table S1.** Classification of bacterial OTUs from Figure 3 (Experiment II).

**Supplemental Table S2.** Classification of bacterial OTUs from Figure 5 (Experiment III).

**Supplemental Table S3.** Classification of fungal OTUs from Figure 6 (Experiment III).

**Supplemental Table S4.** Classification of bacterial OTUs from Figure 7 (Experiment IV).

**Supplemental Table S5.** Classification of fungal OTUs from Figure 8 (Experiment IV).

**Supplemental Figure S1.** Gene expression of *TaMATE1* family at the root apices of *NIL-null* and *NIL-TaMATE1B* wheat lines.

**Supplemental Figure S2.** Testing the  $Al^{3+}$  toxicity of different acidic soils with root growth assays.

**Supplemental Figure S3.** Final shoot dry weight (DW) of wheat plants in Experiment III.

**Supplemental Figure S4.** Final shoot DW of wheat plants in Experiment IV.

**Supplemental Figure S5.** Microbiome structures on wheat roots grown in two different soils.

**Supplemental Figure S6.** Bacterial and fungal microbiome structures on different root tissues of wheat grown in two different soils.

**Supplemental Figure S7.** Relative abundance of the bacterial taxa on different wheat root tissues grown in two different soils.

**Supplemental Figure S8.** Relative abundance of the fungal taxa on different wheat root tissues grown in two different soils.

**Supplemental Figure S9.** Effect of *TaMATE1B* activity on the bacterial and fungal microbiomes on wheat roots grown in the Red Chromosol.

**Supplemental Figure S10.** Effect of *TaMATE1B* activity in combination with *TaALMT1* activity on the bacterial and fungal microbiomes on wheat roots grown in the Ferrosol.

### Acknowledgments

We are grateful to Dr Hanmei Du for technical assistance and Henry Birt for helping to upload the sequences and metadata.

### Funding

This study was supported by an award of a CSIRO Office of the Chief Executive post-doctoral fellowship to A.K.

*Conflict of interest statement.* None declared.

### References

- Antranikian G, Friese C, Quentmeier A, Hippe H, Gottschalk G** (1984) Distribution of the ability for citrate utilization amongst Clostridia. *Arch Microbiol* **138**: 179–182
- Bacilio-Jiménez M, Aguilar-Flores S, Ventura-Zapata E, Pérez-Campos E, Bouquelet S, Zenteno E** (2003) Chemical characterization of root exudates from rice (*Oryza sativa*) and their effects on the chemotactic response of endophytic bacteria. *Plant Soil* **249**: 271–277
- Badri DV, Loyola-Vargas VM, Broeckling CD, De-la-Pena C, Jasinski M, Santelia D, Martinoia E, Sumner LW, Banta LM, Stermitz F, et al.** (2008) Altered profile of secondary metabolites in the root exudates of Arabidopsis ATP-binding cassette transporter mutants. *Plant Physiol* **146**: 762–771
- Bais HP, Weir TL, Perry LG, Gilroy S, Vivanco JM** (2006) The role of root exudates in rhizosphere interactions with plants and other organisms. *Annu Rev Plant Biol* **57**: 233–266
- Baldani JJ, Rouws L, Cruz LM, Olivares FL, Schmid M, Hartmann A** (2014) The family *Oxalobacteraceae*. In E Rosenberg, E DeLong, S Lory, E Stackebrandt, F Thompson, eds, *The Prokaryotes – Alphaproteobacteria and Betaproteobacteria*. Springer, Berlin, Heidelberg, pp 919–974
- Beckers B, De Beeck MO, Thijs S, Truyens S, Weyens N, Boerjan W, Vangronsveld J** (2016) Performance of 16s rDNA primer pairs in the study of rhizosphere and endosphere bacterial microbiomes in metabarcoding studies. *Front Microbiol* **7**: 650
- Beneduzi A, Ambrosini A, Passaglia LMP** (2012) Plant growth-promoting rhizobacteria (PGPR): Their potential as antagonists and biocontrol agents. *Genet Mol Biol* **35**: 1044–1051
- Bengtsson-Palme J, Ryberg M, Hartmann M, Branco S, Wang Z, Godhe A, De Wit P, Sánchez-García M, Ebersberger I, de Sousa F, et al.** (2013) Improved software detection and extraction of ITS1 and ITS2 from ribosomal ITS sequences of fungi and other eukaryotes for analysis of environmental sequencing data. *Methods Ecol Evol* **4**: 914–919
- Bolyen E, Rideout JR, Dillon MR, Bokulich NA, Abnet CC, Al-Ghalith GA, Alexander H, Alm EJ, Arumugam M, Asnicar F, et al.** (2019) Reproducible, interactive, scalable and extensible microbiome data science using QIIME 2. *Nat Biotechnol* **37**: 852–857
- Bulgarelli D, Garrido-Oter R, Munch PC, Weiman A, Droge J, Pan Y, McHardy AC, Schulze-Lefert P** (2015) Structure and function of the bacterial root microbiota in wild and domesticated barley. *Cell Host Microbe* **17**: 392–403
- Bulgarelli D, Rott M, Schlaeppi K, van Themaat EVL, Ahmadinejad N, Assenza F, Rauf P, Huettel B, Reinhardt R, Schmelzer E, et al.** (2012) Revealing structure and assembly cues for *Arabidopsis* root-inhabiting bacterial microbiota. *Nature* **488**: 91–95
- Castro-Sowinski S, Herschkovitch Y, Okon Y, Jurkevitch E** (2007) Effects of inoculation with plant growth-promoting rhizobacteria on resident rhizosphere microorganisms. *FEMS Microbiol Lett* **276**: 1–11
- Chaluvadi S, Bennetzen JL** (2018) Species-associated differences in the below-ground microbiomes of wild and domesticated *Setaria*. *Front Plant Sci* **9**: 1183
- Chevrot R, Rosen R, Haudecoeur E, Cirou A, Shelp BJ, Ron E, Faure D** (2006) GABA controls the level of quorum-sensing signal in *Agrobacterium tumefaciens*. *Proc Natl Acad Sci USA* **103**: 7460–7464

- Cotton TEA, Pétriaccq P, Cameron DD, Meselmani MA, Schwarzenbacher R, Rolfe SA, Ton J (2019) Metabolic regulation of the maize rhizobiome by benzoxazinoids. *ISME J* **13**: 1647–1658
- Deaker R, Roughley RJ, Kennedy IR (2004) Legume seed inoculation technology—a review. *Soil Biol Biochem* **36**: 1275–1288
- Delhaize E, Gruber BD, Ryan PR (2007) The roles of organic anion permeases in aluminium resistance and mineral nutrition. *FEBS Lett* **581**: 2255–2262
- Dennis PG, Hirsch PR, Smith SJ, Taylor RG, Valsami-Jones E, Miller AJ (2009) Linking rhizoplane pH and bacterial density at the microhabitat scale. *J Microbiol Methods* **76**: 101–104
- Dennis PG, Miller AJ, Hirsch PR (2010) Are root exudates more important than other sources of rhizodeposits in structuring rhizosphere bacterial communities? *FEMS Microbiol Ecol* **72**: 313–327
- Edgar RC (2010) Search and clustering orders of magnitude faster than BLAST. *Bioinformatics* **26**: 2460–2461
- Edgar RC (2013) UPARSE: highly accurate OTU sequences from microbial amplicon reads. *Nat Methods* **10**: 996–998
- Han C, Zhang P, Ryan PR, Rathjen TM, Yan Z, Delhaize E (2016) Introgression of genes from bread wheat enhances the aluminium tolerance of durum wheat. *Theor Appl Genet* **129**: 729–739
- Huang AC, Jiang T, Liu YX, Bai YC, Reed J, Qu B, Goossens A, Nützmann HW, Bai Y, Osbourn A (2019) A specialized metabolic network selectively modulates *Arabidopsis* root microbiota. *Science* **364**: eaau6389
- Ihrmark K, Bodeker ITM, Cruz-Martinez K, Friberg H, Kubartova A, Schenck J, Strid Y, Stenlid J, Brandstrom-Durling M, Clemmensen KE, Lindahl BD (2012) New primers to amplify the fungal ITS2 region – evaluation by 454-sequencing of artificial and natural communities. *FEMS Microbiol Ecol* **82**: 666–677
- Kawasaki A, Dennis PG, Forstner C, Raghavendra AKH, Richardson AE, Watt M, Mathesius U, Gilliam M, Ryan PR (2021) The microbiomes on the roots of wheat (*Triticum aestivum* L.) and rice (*Oryza sativa* L.) exhibit significant differences in structure between root types and along root axes. *Funct Plant Biol* **48**: 871–888
- Kawasaki A, Donn S, Ryan PR, Mathesius U, Devilla R, Jones A, Watt M (2016) Microbiome and exudates of the root and rhizosphere of *Brachypodium distachyon*, a model for wheat. *PLoS One* **11**: e0164533
- Kawasaki A, Okada S, Zhang C, Delhaize E, Mathesius U, Richardson AE, Watt M, Gilliam M, Ryan PR (2018) A sterile hydroponic system for characterising root exudates from specific root types and whole-root systems of large crop plants. *Plant Methods* **14**: 114
- Kawasaki A, Ryan PR (2021) Peptide nucleic acid (PNA) clamps to reduce co-amplification of plant DNA during PCR amplification of 16S rRNA genes from endophytic bacteria. In LC Carvalhais, PG Dennis, eds, *The Plant Microbiome: Methods and Protocols*, Springer US, New York, NY, pp 123–134
- Kinraide TB, Parker DR (1989) Assessing the phytotoxicity of mononuclear hydroxy-aluminum. *Plant Cell Environ* **12**: 479–487
- Kochian LV (1995) Cellular mechanisms of aluminum toxicity and resistance in plants. *Annu Rev Plant Physiol Plant Mol Biol* **46**: 237–260
- Koprivova A, Schuck S, Jacoby RP, Klinkhammer I, Welter B, Leson L, Martyn A, Nauen J, Grabenhorst N, Mandelkowitz JF, et al. (2019) Root-specific camalexin biosynthesis controls the plant growth-promoting effects of multiple bacterial strains. *Proc Natl Acad Sci* **116**: 15735–15744
- Kudoyarova G, Arkhipova T, Korshunova T, Bakaeva M, Loginov O, Dodd IC (2019) Phytohormone mediation of interactions between plants and non-symbiotic growth promoting bacteria under edaphic stresses. *Front Plant Sci* **10**: 1368
- Legendre P, Gallagher ED (2001) Ecologically meaningful transformations for ordination of species data. *Oecologia* **129**: 271–280
- Liu J, Xu M, Estavillo GM, Delhaize E, White RG, Zhou M, Ryan PR (2018) Altered expression of the malate-permeable anion channel OsALMT4 reduces the growth of rice under low radiance. *Front Plant Sci* **9**: 542
- Liu J, Zhou M, Delhaize E, Ryan PR (2017) Altered expression of a malate-permeable anion channel, OsALMT4, disrupts mineral nutrition. *Plant Physiol* **175**: 1745–1759
- Love MI, Huber W, Anders S (2014) Moderated estimation of fold change and dispersion for RNA-seq data with DESeq2. *Genome Biol* **15**: 550
- Ma JF, Ryan PR, Delhaize E (2001) Aluminium tolerance in plants and the complexing role of organic acids. *Trends Plant Sci* **6**: 273–278
- McDonald D, Clemente JC, Kuczynski J, Rideout JR, Stombaugh J, Wendel D, Wilke A, Huse S, Hufnagle J, Meyer F, et al. (2012) The Biological Observation Matrix (BIOM) format or: how I learned to stop worrying and love the ome-ome. *GigaScience* **1**: 7
- McMurdie PJ, Holmes S (2013) phyloseq: an R package for reproducible interactive analysis and graphics of microbiome census data. *PLoS One* **8**: e61217
- McMurdie PJ, Holmes S (2014) Waste not, want not: Why rarefying microbiome data is inadmissible. *PLoS Comput Biol* **10**: e1003531
- Mohanram S, Kumar P (2019) Rhizosphere microbiome: revisiting the synergy of plant-microbe interactions. *Ann Microbiol* **69**: 307–320
- Mönchgesang S, Strehmel N, Schmidt S, Westphal L, Taruttis F, Müller E, Herklotz S, Neumann S, Scheel D (2016) Natural variation of root exudates in *Arabidopsis thaliana*-linking metabolomic and genomic data. *Sci Rep* **6**: 29033
- Morita S, Abe J (1994) Modeling root system morphology in rice. In TD Davis, BE Haissig, eds, *Biology of Adventitious Root Formation*, Vol. 62. Springer, Boston, MA, pp 191–202
- Nilsson RH, Glöckner FO, Saar I, Tedersoo L, Kõljalg U, Abarenkov K, Larsson KH, Taylor AFS, Bengtsson-Palme J, Schigel D, et al. (2019) The UNITE database for molecular identification of fungi: handling dark taxa and parallel taxonomic classifications. *Nucleic Acids Res* **47**: D259–D264
- Oburger E, Kirk GJD, Wenzel WW, Puschenreiter M, Jones DL (2009) Interactive effects of organic acids in the rhizosphere. *Soil Biol Biochem* **41**: 449–457
- Oger PM, Mansouri H, Nesme X, Dessaux Y (2004) Engineering root exudation of lotus toward the production of two novel carbon compounds leads to the selection of distinct microbial populations in the rhizosphere. *Microb Ecol* **47**: 96–103
- Oksanen J, Blanchet FG, Friendly M, Kindt R, Legendre P, McGinn D, Minchin PR, O'Hara RB, Simpson GL, Solymos P, et al. (2019) *vegan*: Community Ecology Package. R package version 2.5-6. <https://CRAN.R-project.org/package=vegan>
- Padilla FM, Gallardo M, Manzano-Agugliaro F (2018) Global trends in nitrate leaching research in the 1960-2017 period. *Sci Total Environ* **643**: 400–413
- Pii Y, Mimmo T, Tomasi N, Terzano R, Cesco S, Crecchio C (2015) Microbial interactions in the rhizosphere: beneficial influences of plant growth-promoting rhizobacteria on nutrient acquisition process. A review. *Biol Fertil Soils* **51**: 403–415
- Piñeros MA, Cañado GMA, Kochian LV (2008) Novel properties of the wheat aluminum tolerance organic acid transporter (TaALMT1) revealed by electrophysiological characterization in *Xenopus* oocytes: Functional and structural implications. *Plant Physiol* **147**: 2131–2146
- Quast C, Pruesse E, Yilmaz P, Gerken J, Schweer T, Yarza P, Peplies J, Glockner FO (2013) The SILVA ribosomal RNA gene database project: improved data processing and web-based tools. *Nucleic Acids Res* **41**: D590–D596
- Quentmeier A, Antranikian G (1985) Characterization of citrate lyase from *Clostridium sporosphaeroides*. *Arch Microbiol* **141**: 85–90
- R Core Team. (2019) *R: A Language and Environment for Statistical Computing*. R Core Team, Vienna, Austria.
- Raman H, Ryan PR, Raman R, Stodart BJ, Zhang K, Martin P, Wood R, Sasaki T, Yamamoto Y, Mackay M, et al. (2008)



- Analysis of *TaALMT1* traces the transmission of aluminum resistance in cultivated common wheat (*Triticum aestivum* L.). *Theor Appl Genet* **116**: 343–354
- Ramesh SA, Kamran M, Sullivan W, Chirkova L, Okamoto M, Degryse F, McLaughlin M, Gilliam M, Tyerman SD** (2018) Aluminum-activated malate transporters can facilitate GABA transport. *Plant Cell* **30**: 1147–1164
- Ramesh SA, Tyerman SD, Xu B, Bose J, Kaur S, Conn V, Domingos P, Ullah S, Wege S, Shabala S, et al.** (2015) GABA signalling modulates plant growth by directly regulating the activity of plant-specific anion transporters. *Nat Commun* **6**: 7879
- Rudrappa T, Czymbek KJ, Pare PW, Bais HP** (2008) Root-secreted malic acid recruits beneficial soil bacteria. *Plant Physiol* **148**: 1547–1556
- Rüger L, Feng K, Dumack K, Freudenthal J, Chen Y, Sun R, Wilson M, Yu P, Sun B, Deng Y, et al.** (2021) Assembly patterns of the rhizosphere microbiome along the longitudinal root axis of maize (*Zea mays* L.). *Front Microbiol* **12**: 614501
- Ryan PR, Delhaize E** (2010) The convergent evolution of aluminium resistance in plants exploits a convenient currency. *Funct Plant Biol* **37**: 275–284
- Ryan PR, Delhaize E, Randall PJ** (1995) Characterization of Al-stimulated efflux of malate from the apices of Al-tolerant wheat roots. *Planta* **196**: 103–110
- Ryan PR, Dessaux Y, Thomashow LS, Weller DM** (2009a) Rhizosphere engineering and management for sustainable agriculture. *Plant Soil* **321**: 363–383
- Ryan PR, Raman H, Gupta S, Horst WJ, Delhaize E** (2009b) A second mechanism for aluminum resistance in wheat relies on the constitutive efflux of citrate from roots. *Plant Physiol.* **149**: 340–351
- Sasaki T, Ryan PR, Delhaize E, Hebb DM, Ogihara Y, Kawaura K, Noda K, Kojima T, Toyoda A, Matsumoto H, et al.** (2006) Sequence upstream of the wheat (*Triticum aestivum* L.) *ALMT1* gene and its relationship to aluminum resistance. *Plant Cell Physiol* **47**: 1343–1354
- Sasaki T, Yamamoto Y, Ezaki B, Katsuhara M, Ahn SJ, Ryan PR, Delhaize E, Matsumoto H** (2004) A wheat gene encoding an aluminum-activated malate transporter. *Plant J* **37**: 645–653
- Sharma T, Dreyer I, Kochian L, Piñeros MA** (2016) The ALMT family of organic acid transporters in plants and their involvement in detoxification and nutrient security. *Front Plant Sci* **7**: 1488
- Soedarjo M, Borthakur D** (1996) Mimosine produced by the tree-legume *Leucaena* provides growth advantages to some *Rhizobium* strains that utilize it as a source of carbon and nitrogen. *Plant Soil* **186**: 87–92
- Strandwitz P, Kim KH, Terekhova D, Liu JK, Sharma A, Levering J, McDonald D, Dietrich D, Ramadhar TR, Lekbua A, et al.** (2019) GABA-modulating bacteria of the human gut microbiota. *Nat Microbiol* **4**: 396–403
- Stringlis IA, Yu K, Feussner K, de Jonge R, Van Bentum S, Van Verk MC, Berendsen RL, Bakker PAHM, Feussner I, Pieterse CMJ** (2018) MYB72-dependent coumarin exudation shapes root microbiome assembly to promote plant health. *Proc Natl Acad Sci USA* **115**: E5213–E5222
- Tawarayama K, Horie R, Shinano T, Wagatsuma T, Saito K, Oikawa A** (2014) Metabolite profiling of soybean root exudates under phosphorus deficiency. *Soil Sci Plant Nutr* **60**: 679–694
- Tesfaye M, Dufault NS, Dornbusch MR, Allan DL, Vance CP, Samac DA** (2003) Influence of enhanced malate dehydrogenase expression by alfalfa on diversity of rhizobacteria and soil nutrient availability. *Soil Biol Biochem* **35**: 1103–1113
- Thapa S, Sotang N, Limbu AK, Joshi A** (2020) Impact of *Trichoderma* sp. in agriculture: A mini-review. *J Biol Today's World* **9**: 227
- Toju H, Tanabe AS, Yamamoto S, Sato H** (2012) High-coverage ITS primers for the DNA-based identification of ascomycetes and basidiomycetes in environmental samples. *PLOS ONE* **7**: e40863
- Tovkach A, Ryan PR, Richardson AE, Lewis DC, Rathjen TM, Ramesh S, Tyerman SD, Delhaize E** (2013) Transposon-mediated alteration of *TaMATE1B* expression in wheat confers constitutive citrate efflux from root apices. *Plant Physiol* **161**: 880–892
- Vessey JK** (2003) Plant growth promoting rhizobacteria as biofertilizers. *Plant Soil* **255**: 571–586
- Voges MJEEE, Bai Y, Schulze-Lefert P, Sattely ES** (2019) Plant-derived coumarins shape the composition of an *Arabidopsis* synthetic root microbiome. *Proc Natl Acad Sci* **116**: 12558–12565
- Walker TS, Bais HP, Grotewold E, Vivanco JM** (2003a) Root exudation and rhizosphere biology. *Plant Physiol* **132**: 44–51
- Walker TS, Bais HP, Halligan KM, Stermitz FR, Vivanco JM** (2003b) Metabolic profiling of root exudates of *Arabidopsis thaliana* J Agric Food Chem **51**: 2548–2554
- Walther R, Hippe H, Gottschalk G** (1977) Citrate, a specific substrate for the isolation of *Clostridium sphenoides*. *Appl Environ Microbiol* **33**: 955–962
- Wang P, Bi SP, Wang S, Ding QY** (2006) Variation of wheat root exudates under aluminum stress. *J Agric Food Chem* **54**: 10040–10046
- Wang Y, Naumann U, Wright ST, Warton DI** (2012) mvabund— an R package for model-based analysis of multivariate abundance data. *Methods Ecol Evol* **3**: 471–474
- Wang Y, Ying H, Yin Y, Zheng H, Cui Z** (2019) Estimating soil nitrate leaching of nitrogen fertilizer from global meta-analysis. *Sci Total Environ* **657**: 96–102
- Warren CR** (2016) Simultaneous efflux and uptake of metabolites by roots of wheat. *Plant Soil* **406**: 359–374
- Weisskopf L, Heller S, Eberl L** (2011) *Burkholderia* species are major inhabitants of white lupin cluster roots. *Appl Environ Microbiol* **77**: 7715–7720
- White TJ, Bruns T, Lee S, Taylor J** (1990) Amplification and direct sequencing of fungal ribosomal RNA genes for phylogenetics. *In* MA Innis, DH Gelfand, JJ Sninsky, TJ White, eds, PCR protocols: a guide to methods and applications, Academic Press, San Diego, pp 315–322
- White LJ, Ge X, Brözel VS, Subramanian S** (2017) Root isoflavonoids and hairy root transformation influence key bacterial taxa in the soybean rhizosphere. *Environ Microbiol* **19**: 1391–1406
- Willems A, De Ley J, Gillis M, Kersters K** (1991) Notes: *Comamonadaceae*, a new family encompassing the acidovorans rRNA complex, including *Variovorax paradoxus* gen. nov., comb. nov., for *Alcaligenes paradoxus* (Davis 1969). *Int J Syst Bacteriol* **41**: 445–450
- Wu L, Kobayashi Y, Wasaki J, Koyama H** (2018) Organic acid excretion from roots: a plant mechanism for enhancing phosphorus acquisition, enhancing aluminum tolerance, and recruiting beneficial rhizobacteria. *Soil Sci Plant Nutr* **64**: 697–704
- Zhang WH, Ryan PR, Sasaki T, Yamamoto Y, Sullivan W, Tyerman SD** (2008) Characterization of the *TaALMT1* protein as an Al<sup>3+</sup>-activated anion channel in transformed tobacco (*Nicotiana tabacum* L.) cells. *Plant Cell Physiol* **49**: 1316–1330
- Zhang Z, Schwartz S, Wagner L, Miller W** (2000) A greedy algorithm for aligning DNA sequences. *J Comput Biol* **7**: 203–214